Nuclear magnitudes and the size distribution of Jupiter family comets

Gonzalo Tancredi [a,*], Julio A. Fernández [a], Hans Rickman [b], Javier Licandro [c,d]

[a] *Departamento de Astronomía, Facultad de Ciencias, Iguá 4225, 11400 Montevideo, Uruguay*
[b] *Astronomiska Observatoriet, Box 515, S-75120 Uppsala, Sweden*
[c] *Isaac Newton Group of Telescopes, P.O. Box 321, Santa Cruz de La Palma, Spain*
[d] *Instituto Astrofísico de Canarias, C/Vía Láctea s/n, 38200 La Laguna, Spain*

Abstract

We present a new catalog of absolute nuclear magnitudes of Jupiter family (JF) comets, which is an updated version of our previous catalog [Tancredi, G., Fernández, J.A., Rickman, H., Licandro, J., 2000. Astron. Astrophys. Suppl. Ser. 146, 73–90]. From the new catalog we find a linear cumulative luminosity function (CLF) of slope 0.54 ± 0.05 for JF comets with $q \lesssim 2.5$ AU. By considering this CLF combined with the few measured geometric albedos with their respective uncertainties, and assuming a canonical albedo of 0.035 ± 0.012 for those comets with undetermined albedos, we derive a cumulative size distribution that follows a power-law of index -2.7 ± 0.3. The slope is similar to that derived from some theoretical collisional models and from some populations of Solar System bodies like the trans-neptunian objects. We also discuss and compare our size distribution with those by other authors that have recently appeared in the literature. Some striking differences in the computed slopes are explained in terms of biases in the studied samples, the different weights given to the brightest members of the samples, and discrepancies in the values of a few absolute nuclear magnitudes. We also compute sizes and fractions of active surface area of JF comets from their estimated absolute nuclear magnitudes and their water production rates. With the outgassing model that we use, about 60% of the computed fractions f of active surface area are found to be smaller than 0.2, with one case (28P/Neujmin 1) of no more than 0.001, which suggests that JF comets may transit through stages of very low activity, or even dormancy. There is an indication that JF comets with radii $R_N \gtrsim 3$ km have active fractions $f \lesssim 0.01$, which might be due to the rapid formation of insulating dust mantles on larger nuclei.

1. Introduction

For some periodic comets we now have fairly good estimates of their nuclear size and albedo. In a few cases this has been possible through flyby missions: 1P/Halley observed by the Giotto and Vega spacecrafts, 19P/Borrelly imaged by the Deep Space 1 mission from a distance as close as about 3400 km, and 81P/Wild 2 imaged by the Stardust spacecraft within a distance of only 236 km. A few other Jupiter family (JF) comets have been observed from the ground in the visible and thermal infrared on occasions when they had little or no activity

at all. An important result is that practically all these comets show very low geometric albedos, mostly in the range $p_V \sim 0.02$–0.06 with an average $p_V \sim 0.04$ (Hartmann et al., 1987; Lamy et al., 2005).

Furthermore, the increased availability of telescopes with large apertures and the introduction of CCD cameras have revolutionized the photometric measurement of comets, which have become possible to observe at ever larger heliocentric distances. We are thus now able to obtain reliable nuclear magnitudes far from the Sun. In addition, high-resolution, space-borne photometric imaging, in particular using the HST (see, e.g., Lamy et al., 2005 for a complete list of their observations), have also provided an important set of nuclear magnitudes for comets closer to the Sun and hence more active, by offering a realistic possibility of coma subtraction.

---

* Corresponding author. Fax: +598 2 525 0580.
E-mail address: gonzalo@fisica.edu.uy (G. Tancredi).

There are several important reasons to investigate the sample of nuclear magnitudes of JF comets. One of them has to do with explaining the dynamical origin of this population. The most likely source region is the trans-neptunian "scattered disk," where several 10^2-km-sized objects have been observed but smaller objects remain undiscovered. In order to fully establish this dynamical link, we need to confront the capture efficiency with both observable lifetimes and realistic estimates of numbers of objects. Since most of the observed JF cometary nuclei have diameters in the 1–10 km range, an extrapolation by means of a well-established size distribution is a necessary prerequisite. It may also be possible, by modeling the physical evolutionary effects on the JF size distribution, to relate the observed slope to the accretional and/or collisional evolution in the source region and, thus, to make some important inferences about cometary formation.

We would also like to learn about the fraction of active surface area, since it has often been argued that comets may build insulating dust mantles that choke off ice sublimation after one or more perihelion passages. Different models for this phenomenon have been proposed by, e.g., Rickman et al. (1990) and Kührt and Keller (1994), with different predictions as to the dependence on perihelion distance or nuclear radius. Statistics on the distribution of active fractions would provide a means to test these models. For this purpose, in addition to the absolute nuclear magnitudes, we may use gas production rates observed when comets are close to perihelion. The availability of a large enough sample of good nuclear magnitudes, a relevant sample of production rates, and reliable information on the distribution of albedos, is a prerequisite for this kind of analysis, and in this paper we will make an attempt—using, for the moment, a very simple model of the H_2O outgassing.

The size distribution of any sample of observed comets is bound to be strongly biased by selection effects. If we look for statistical information representing the entire population, we have to apply algorithms to debias the observed sample. For that purpose, it is also natural to focus on the JF comets. These objects provide the most complete and reliable sample of cometary magnitude estimates. Because of their small orbital periods, most JF comets have been observed through most of their orbits, yielding a large number of magnitudes, some of them far from the Sun, where the comets show a "stellar" appearance without signs of gaseous activity. Observational materials of comparable quality are not available for any other category of comets.

Five years ago we compiled a catalog of nuclear magnitudes of JF comets, based on the set of photometric data that then existed. Some of this was from our own observations, but the majority came from a literature search of the published data on cometary nuclear magnitudes (see Tancredi et al., 2000 for a list of used sources). Using a debiasing technique, a size distribution was derived from these data. We now return to the problem again, since the number of good observations of cometary nuclear magnitudes has continued to increase steadily, so our new catalog, presented here, is a real improvement over the previous one. We are also able this time to make comparisons with recent efforts by other authors, and to pay more attention to the

role of the assumed albedos. We shall thus re-analyze the problem of nuclear sizes and the size distribution of JF comets. As a byproduct, we will use the new derived sizes to estimate fractions of active surface area.

2. Definition of populations

A critical point when analyzing a given population of objects is to precisely define the common characteristics that distinguish its members. The definition of the Jupiter family of comets has recently experienced several adjustments, which we will now discuss. Let us start with the almost arbitrary classification into short-period comets as objects with periods less than 20 years, intermediate-period ones between 20 and 200 years and long-period comets with periods larger than 200 years. This is the classification still in use by the IAU Minor Planet Center (MPC). These groups show other dynamical differences beside the period. While intermediate- and long-period comets present a mixture of prograde and retrograde orbits, short-period comets have only prograde ones. In the 1980's, this led to the speculation that these populations may have different source regions: the intermediate-period comets came from the Oort cloud, while the short-period comets came from an, at that moment putative, trans-neptunian (TN) belt (Fernández, 1980; Duncan et al., 1988). This proposal was later confirmed by the discovery of trans-neptunian objects (TNOs) and different numerical simulations that described the process of transfer from the TN belt to the visible region (Levison and Duncan, 1997).

Another difference comes from the effect of Jupiter in the orbital evolution: while most of the short-period comets have low encounter velocities with the planet, the intermediate-period ones have much larger encounter velocities. This difference is expressed by the values of the Tisserand parameter, which is defined as

$$T = \frac{a_J}{a} + 2\sqrt{\frac{a}{a_J}(1 - e^2)}\cos i, \qquad (1)$$

where a, e, and i are the semimajor axis, eccentricity, and inclination of the comet, and a_J is the radius of Jupiter's orbit, assumed to be circular. The Tisserand parameter is related to the encounter velocity at infinity, i.e., outside Jupiter's gravitational potential well, U (in the circular restricted three-body problem), by $U = \sqrt{3 - T}$, expressing U in terms of Jupiter's orbital velocity.

Almost all the short-period comets have T between 2 and 3, while almost all the intermediate-period ones have values lower than 2, even including negative values. Like the above-mentioned characteristic feature of the inclinations, this difference can be understood in the framework of the different evolutions from the source regions into the inner Solar System. The transfer of control from an outer planet to the next inner one (the "handing down" process) generally involves low-velocity encounters and therefore T-values close to 3 with respect to the planet in question. In the circular restricted three-body problem, orbits with $T > 3$ cannot cross the orbit of the planet. But in reality, where Jupiter has a slight eccentricity, values of T just above 3 still allow the objects to encounter the planet. To define

a precise limit is beyond the scope of this paper, but we can be confident that orbits with $T \gtrsim 3.1$ do not allow encounters with Jupiter in the short term.

More recently another criterion has been considered. Some comets and asteroids have been discovered in orbits entirely outside Jupiter's orbit, most of them crossing the orbits of the other giant planets. This family of objects has been named centaurs. Some of them show a clear cometary activity (e.g., 29P/Schwassmann–Wachmann 1 and 95P/Chiron) or indications that ice may exist at or very close to the surface. The very low temperatures at those distances and possibly the depletion of the most volatile ices is then expected to prevent any activity. Most of these objects are supposed to be in the process of transfer from the trans-neptunian belt to the inner Solar System. In contrast to the vast majority of the short-period comets, these objects are not yet experiencing strong perturbations caused by encounters with Jupiter. Furthermore, since most of the centaurs have been discovered in recent years, the sample is affected by important problems of incompleteness. In particular, for objects smaller than ∼30 km, there are very few discoveries and the degree of incompleteness of the sample should be very high.

Carusi et al. (1987) and Valsecchi (1992) introduced a classification of Jupiter family and Halley-type comets in terms of the Tisserand parameter. They defined Halley-type comets as those having $20 < P < 200$ yr and $T < 2$, whereas Jupiter family comets have $P < 20$ yr and $T > 2$. More recently, Levison (1996) defined "ecliptic comets" as those with $T > 2$ and "nearly isotropic" ones as those with $T < 2$. Among the ecliptic comets he considered the Jupiter family to be the objects with $T < 3$, while he separated the Encke-types ($T > 3$ and $a < a_J$) and the Chiron-types ($T > 3$ and $a > a_J$) as special groups.

Let us point out a few weaknesses of these classifications. Carusi et al.'s proposal still maintains the somewhat arbitrary limit at $P = 20$ yr, which is not sustained by any dynamical consideration. Levison's sub-classification of the ecliptic comets created two new groups with one single object each (2P/Encke and 95P/Chiron).[1] Though 2P/Encke is dynamically distinct from the other JF comets, since its orbit is completely inside the orbit of Jupiter and detached from strong interactions with the planet, this must clearly be due to the action of special effects such as persistent non-gravitational forces for a long period of time (e.g., Fernández et al., 2002) or a close encounter with a terrestrial planet. In the case of the Chiron-type group, let us point out that objects with $T < 3$ and orbits completely outside Jupiter's orbit, avoiding strong interactions, are still possible (e.g., an orbit with $T = 3$, $a = 30$ AU, and $i = 0°$ has $q = 5.75$ AU).

We will introduce a slightly different classification based on the previous considerations: we define *Jupiter family* comets as objects with $2 < T \lesssim 3.1$ and $q < Q_J$ (Q_J is Jupiter's aphelion distance); and *centaur* comets as objects—some of which show gas and dust activity—that fulfill the criteria $q > Q_J$ and

$a < a_N$ (a_N is Neptune's semimajor axis). According to current thinking about cometary dynamics, a Jupiter family with this definition should be rather homogeneous with regard to formation conditions and past evolution, whereas the risk of admixture with objects with quite a different history would increase sharply, if we would include comets with $T < 2$, and severe effects of observational bias are likely, if we include centaur comets.

3. Photometric data: An updated version

We have earlier produced a catalog of absolute nuclear magnitudes of Jupiter family comets (Tancredi et al., 2000) (from here on T00). The same list of sources to look for published data has been used: i.e., peer-reviewed journals with detailed studies of a single or a few comets, magnitudes reported to the MPC or International Comet Quarterly (the vast majority of the data), the Cometary Light Curve Catalog (CLICC) by Kamél (1991). New nuclear magnitudes were transformed to absolute nuclear magnitudes (H_N) in the same manner as in T00. Our catalog may be taken as a first step for deriving a good set of absolute nuclear magnitudes, understood to be the true magnitudes of the bare nuclei. This has been a very controversial issue, and many authors argued about the near impossibility to resolve the nucleus from the coma. However, when JF comets are observed near aphelion with large telescopes, there is a good chance that the determined magnitudes get close to the true nuclear magnitudes, as the comets decrease their activity and may become nearly inactive. We have updated the T00 catalog, which was based on data through August 1998, with more recent data from other authors and from our own observing runs.

An updated list of absolute nuclear magnitudes is shown in Table 1, based on observations through December 31, 2002. We note that the names of the comets in all tables are given without the sequential numbers otherwise used for unambiguous identification (e.g., Comets 9P/Tempel and 10P/Tempel instead of Tempel 1 and Tempel 2), in agreement with the IAU naming rules. The new version of the catalog can be accessed on line at http://www.fisica.edu.uy/~gonzalo/catalog. Since the publication of our first catalogue, the amount of data on nuclear magnitudes has greatly increased. We refer in particular to the large sets of nuclear magnitudes obtained by three different research groups: Lowry et al. (2003) (hereafter Lo03), Lamy et al. (2005) (hereafter La05), and Meech et al. (2004) (hereafter Me04). The values of the nuclear radius R_N listed in Table 1 have been computed from the corresponding H_N values using Eq. (3) and assuming a standard albedo $p_V = 0.04$.

In the same way as in T00, we have generally adopted as the true nuclear magnitude a mean among the fainter observations reported with a stellar appearance ("nuclear magnitudes" in the sense used by the MPC). This has led several authors to criticize our adopted nuclear magnitudes, because we have included data in our catalog from many different sources, in particular magnitudes reported to the MPC by amateur astronomers and inexperienced observers. In order to make an estimate of the adopted nuclear magnitude, we discuss in detail comet by comet and analyze the sources for the most relevant data points to evaluate

---

[1] Since the publication of Levison's (1996) classification scheme, several Chiron-type comets have been discovered, like: 165P/LINEAR, 166P/NEAT, 167P/CINEOS, and P/2004A1 (LONEOS).

Table 1
Absolute nuclear magnitudes of JF comets

Comet	H_N	QC	R_N (km)	H_N (T00)	QC (T00)
2P/Encke	16.0	3	2.10	17.0	3
4P/Faye	16.3	1	1.83	15.9	2
6P/d'Arrest	16.5	1	1.66	16.7	2
7P/Pons–Winnecke	16.3	3	1.83	16.8	3
9P/Tempel	15.6	1	2.52	15.8	1
10P/Tempel	14.9	2	3.48	15.3	2
14P/Wolf	16.2	4	1.91	17.0	4
15P/Finlay	17.2	4	1.21	17.9	4
16P/Brooks	16.6	4	1.59	16.5	3
17P/Holmes	16.6	1	1.59	16.1	3
19P/Borrelly	15.9	1	2.19	15.2	1
21P/Giacobini–Zinner	17.6	3	1.00	17.7	2
22P/Kopff	16.3	1	1.83	16.3	2
24P/Schaumasse	17.8	4	0.91	18.0	4
26P/Grigg–Skjellerup	17.2	1	1.21	17.1	1
28P/Neujmin	12.7	1	9.58	12.8	1
30P/Reinmuth	17.6	3	1.00	17.1	3
31P/Schwassmann–Wachmann	15.2	2	3.03	15.1	1
32P/Comas–Solá	15.6	3	2.52	15.6	3
33P/Daniel	17.8	4	0.91	17.9	4
36P/Whipple	16.0	1	2.10	15.8	2
37P/Forbes	17.6	2	1.00	17.6	3
40P/Väisälä	16.5	3	1.66	16.7	3
41P/Tuttle–Giacobini–Kresák	18.4	4	0.69	18.5	3
42P/Neujmin	18.4	4	0.69	18.7	4
43P/Wolf–Harrington	16.0	2	2.10	16.3	2
44P/Reinmuth	16.7	3	1.52	16.8	4
45P/Honda–Mrkos–Pajdušáková	20.0	3	0.33	19.3	4
46P/Wirtanen	18.8	1	0.58	18.4	1
47P/Ashbrook–Jackson	15.5	1	2.64	15.3	1
48P/Johnson	15.9	2	2.19	15.9	2
49P/Arend–Rigaux	14.8	1	3.64	15.1	1
50P/Arend	17.7	4	0.96	15.2	4
51P/Harrington	20.8	4	0.23	16.9	4
52P/Harrington–Abell	17.4	4	1.10	17.4	4
53P/Van Biesbroeck	15.0	1	3.32	14.7	3
56P/Slaughter–Burnham	16.8	1	1.45	16.7	3
58P/Jackson–Neujmin	18.7	4	0.60	18.7	4
59P/Kearns–Kwee	17.6	3	1.00	18.2	3
60P/Tsuchinshan	18.4	4	0.69	18.2	3
61P/Shajn–Schaldach	18.0	2	0.83	17.5	3
62P/Tsuchinshan	–	–	–	18.1	4
63P/Wild	16.8	2	1.45	–	–
64P/Swift–Gehrels	16.3	4	1.83	16.4	4
65P/Gunn	14.3	2	4.59	14.2	2
67P/Churyumov–Gerasimenko	16.0	1	2.10	15.6	1
68P/Klemola	15.6	3	2.52	15.9	3
69P/Taylor	16.0	4	2.10	–	–
70P/Kojima	17.1	3	1.26	17.3	3
71P/Clark	18.0	2	0.83	17.1	2
73P/Schwassmann–Wachmann	17.7	3	0.96	17.7	4
74P/Smirnova–Chernykh	15.1	3	3.17	13.7	4
75P/Kohoutek	16.3	3	1.83	16.3	3
76P/West–Kohoutek–Ikemura	–	–	–	17.1	3
77P/Longmore	15.8	4	2.30	15.7	4
78P/Gehrels	16.4	3	1.74	16.0	3
79P/du Toit–Hartley	17.2	4	1.21	–	–
81P/Wild	16.2	2	1.91	15.9	3
82P/Gehrels	18.1	3	0.80	16.1	2
67P/Churyumov–Gerasimenko	16.0	1	2.10	15.6	1
68P/Klemola	15.6	3	2.52	15.9	3
69P/Taylor	16.0	4	2.10	–	–
70P/Kojima	17.1	3	1.26	17.3	3
71P/Clark	18.0	2	0.83	17.1	2

Table 1 (*continued*)

| Comet	H_N	QC	R_N (km)	H_N (T00)	QC (T00)
73P/Schwassmann–Wachmann	17.7	3	0.96	17.7	4
74P/Smirnova–Chernykh	15.1	3	3.17	13.7	4
75P/Kohoutek	16.3	3	1.83	16.3	3
76P/West–Kohoutek–Ikemura	–	–	–	17.1	3
77P/Longmore	15.8	4	2.30	15.7	4
78P/Gehrels	16.4	3	1.74	16.0	3
79P/du Toit–Hartley	17.2	4	1.21	–	–
81P/Wild	16.2	2	1.91	15.9	3
82P/Gehrels	18.1	3	0.80	16.1	2
84P/Giclas	17.5	3	1.05	16.9	4
86P/Wild	19.0	2	0.53	17.8	3
87P/Bus	19.0	4	0.53	17.1	3
88P/Howell	17.7	4	0.96	17.4	3
89P/Russell	17.3	4	1.15	17.4	3
90P/Gehrels	15.5	3	2.64	15.4	4
91P/Russell	17.1	4	1.26	17.1	4
92P/Sanguin	17.2	2	1.21	–	–
94P/Russell	16.1	3	2.00	16.2	3
97P/Metcalf–Brewington	16.8	4	1.45	17.0	4
98P/Takamizawa	15.3	4	2.89	15.7	4
99P/Kowal	14.2	3	4.80	14.2	3
100P/Hartley	–	–	–	17.1	3
101P/Chernykh	15.9	3	2.19	15.9	3
103P/Hartley	17.2	3	1.21	14.7	4
104P/Kowal	16.8	4	1.45	–	–
105P/Singer–Brewster	18.0	4	0.83	17.7	4
106P/Schuster	18.0	3	0.83	–	–
108P/Ciffréo	18.0	3	0.83	–	–
110P/Hartley	16.1	2	2.00	16.2	2
111P/Helin–Roman–Crockett	17.3	4	1.15	16.7	3
112P/Urata–Niijima	18.2	3	0.76	18.4	4
113P/Spitaler	17.3	3	1.15	17.4	4
114P/Wiseman–Skiff	17.9	3	0.87	–	–
116P/Wild	15.0	4	3.32	14.9	3
117P/Helin–Roman–Alu	14.8	3	3.64	14.9	2
118P/Shoemaker–Levy	16.2	3	1.91	16.6	3
119P/Parker–Hartley	16.3	3	1.83	15.6	4
120P/Mueller	18.0	4	0.83	18.1	3
121P/Shoemaker–Holt	16.1	4	2.00	–	–
123P/West–Hartley	16.1	3	2.00	15.9	4
124P/Mrkos	16.4	2	1.74	16.6	2
125P/Spacewatch	18.0	3	0.83	18.0	2
128P/Shoemaker–Holt	16.1	3	2.00	16.1	4
129P/Shoemaker–Levy	16.5	4	1.66	–	–
130P/McNaught–Hughes	16.6	3	1.59	16.5	3
131P/Mueller	18.1	4	0.80	18.2	4
132P/Helin–Roman–Alu	–	–	–	17.8	4
134P/Kowal–Vávrová	16.8	3	1.45	16.9	3
135P/Shoemaker–Levy	16.9	3	1.38	16.8	3
136P/Mueller	–	–	–	16.2	4
137P/Shoemaker–Levy	15.4	2	2.76	15.3	2
138P/Shoemaker–Levy	–	–	–	18.0	4
143P/Kowal–Mrkos	14.3	3	4.59	–	–
144P/Kushida	17.3	3	1.15	17.3	3
147P/Kushida–Muramatsu	–	–	–	15.8	3
152P/Helin–Lawrence	16.0	3	2.10	14.3	4
154P/Brewington	16.5	4	1.66	16.8	4
P/1993 W1 (Mueller)	–	–	–	16.0	4
P/1994 J3 (Shoemaker)	–	–	–	15.0	4
P/1995 A1 (Jedicke)	15.2	3	3.03	15.2	3
P/1996 A1 (Jedicke)	14.1	2	5.03	14.1	2
P/1997 C1 (Gehrels)	15.6	3	2.52	15.6	4
P/1997 G1 (Montani)	15.5	4	2.64	15.6	4
P/1997 V1 (Larsen)	–	–	–	14.8	4
P/2002 BV (Yeung)	15.0	4	3.32	–	–
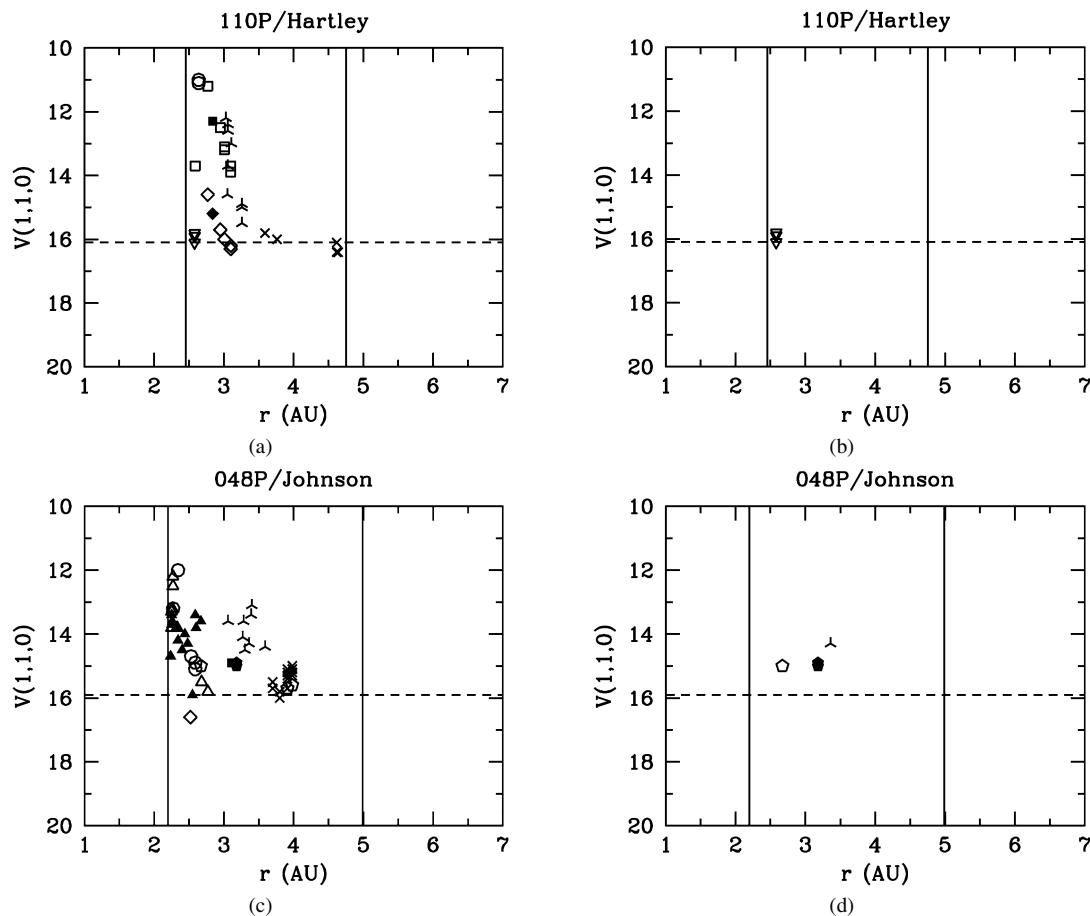
Fig. 1. Plots of the observed absolute magnitudes as a function of the observed heliocentric distances for two comets: (a) all the data for Comet 110P/Hartley, (b) peer-reviewed data for Comet 110P/Hartley, (c) same as (a) for Comet 48P/Johnson, (d) same as (b) for Comet 48P/Johnson. The symbols correspond to different groups of observers as explained in Table 2. The horizontal dashed line corresponds to the derived nuclear magnitude for each comet as it is presented in Table 1.

the quality of the data. We also analyze the consistency between the different observations in order to derive an absolute nuclear magnitude and define a quality class. We look for magnitudes measured by different observers at different heliocentric distances and agreement among the faintest magnitudes measured at different heliocentric distances. We give a higher weight in our analysis to data coming from detailed studies, generally published in peer-reviewed journals. Nevertheless, we do not completely disregard, as the other groups have done, the rest of the data points, since we consider that some such observations may in fact stand a chance to witness the true bare nucleus.

The relevance of taking into account all the available data is shown in the following examples. From the complete data set, let us extract the data that was published in peer-reviewed journals. In Fig. 1 we show plots for two comets, both with all the available data and with the peer-reviewed data only: (a) all the data for Comet 110P/Hartley, (b) peer-reviewed data for Comet 110P/Hartley, (c) same as (a) for Comet 48P/Johnson, (d) same as (b) for Comet 48P/Johnson. The observed absolute magnitudes (reduced as it is explained in T00) are plotted versus the observed heliocentric distances. The symbols correspond to different groups of observers as explained in Table 2. The nuclear magnitudes that one can derive for 110P are very similar

Table 2
Symbols used for data points in Fig. 1

Observer	Symbol (pre—empty; post—full)
CCD	Pentagon
Roemer	Upward triangle
Scotti (nuclear)	Diamond
Scotti (total)	Square
Lamy et al.	Downward triangle
General	Circle
Total $r > 3$ AU	Pre—cross
	Post—chicken-foot

whether we consider only the peer-reviewed data (data from Lamy et al.) (Fig. 1b) or the whole data set (Fig. 1a). The consistence of Scotti's coma subtracted magnitudes and other magnitudes taken from the MPC with Lamy et al.'s magnitude give us more confidence in our derived nuclear magnitude, and therefore we can assign to this comet a better quality class (see below for the definition of quality classes). In the case of 48P the derived nuclear magnitude based on the peer-reviewed data is ∼1 mag brighter than the one based on all the available data. There are magnitudes measured by Roemer from photographic plates, a coma subtracted magnitude by Scotti as well as

a large set of magnitudes taken from the MPC that are in mutual agreement and these are much fainter than the peer-reviewed data.

Also like in T00, we have classified our absolute nuclear magnitudes H_N into *quality classes* (QC) according to the estimated uncertainty in the adopted H_N, namely: QC 1 are those with an estimated uncertainty less than ±0.3 mag; QC 2 those with uncertainties between ±0.3 and ±0.6 mag; QC 3 those with uncertainties between ±0.6 and ±1 mag, and QC 4 are those with uncertainties between ±1 and ±1.5 mag, although in some cases the estimated magnitudes can only be considered as upper limits to the true nuclear brightness. Note that these uncertainties for the different quality classes yield the following relative errors in the radius estimates: QC 1—<6%, QC 2—6–12%, QC 3—12–20%, and QC 4—20–30%. Our new catalog contains 105 JF comets with the following distribution over the quality classes: 15 (QC 1), 16 (QC 2), 41 (QC 3), and 33 (QC 4). Let us note that comets with QC 4 are generally excluded from further analysis.

We eliminated 12 comets from T00: eight of those were classified as QC 4 in T00, and their magnitude records are now considered to be too poor to attempt any estimate. Two other discarded comets are 76P/West–Kohoutek–Ikemura and 147P/Kushida–Muramatsu, which were classified as QC 3 in T00, because single new HST observations by Lamy et al. (2005) give absolute magnitudes more than three units fainter than the faintest ones recorded before. Though we think that these HST observations are of very good quality, we have decided not to rely on single measurements well apart from the rest of the data set for any comet. This is a general guideline but holds in particular when the data was obtained by a complex reduction method like coma subtraction. These two comets may be very small (faint) comets, but we need more observations to settle the issue of the great discrepancy. The two remaining discarded comets are 29P/Schwassmann–Wachmann 1 and 39P/Oterma, which were included into T00 but discarded in the present catalog, because their perihelion distances are greater than the upper limit that we now impose on the definition of a JF comet. The latter comet had a low enough perihelion distance during the three apparitions observed until 1962, but the nuclear magnitudes obtained photographically at that time were much brighter than the recent CCD-based magnitudes, which thus represent the only reliable data but pertain to a comet with too large a perihelion distance.

On the other hand, there are also 11 comets that had to be discarded in T00, but which now have good enough data to be included, and one additional comet that was discovered after T00 was compiled. Hence the number of comets is the same in both catalogs.

Fig. 2 shows a comparison of our updated list of nuclear magnitudes with that of the T00 catalog. We can see that in general the differences between our updated magnitudes and previous ones are not substantial, most of the largest differences arising from comets, whose nuclear magnitudes are and/or were of quality class 4. There is only one comet, 82P/Gehrels 3, classified in T00 and in the present catalog as QC 3 or better, that shows a discrepancy of two magnitudes. New HST
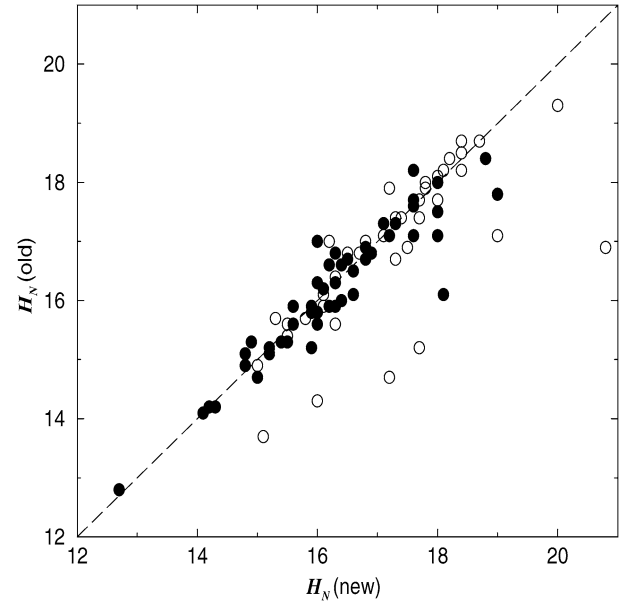

Fig. 2. Our current set of absolute nuclear magnitudes is plotted versus our previous set (Tancredi et al., 2000). Filled circles denote comets that have been classified as QC 1–3 in both sets; open circles are for comets classified as QC 4 in one set or both. The dashed line indicates $H_N(\text{old}) = H_N(\text{new})$.

observations by Lamy et al. show that this comet is fainter than was inferred from the previous data set. Yet we note that, before, Scotti had provided a single coma-subtracted estimate of $H_N = 17.5$, close to Lamy et al.'s HST measurement. In retrospect, we could have had more confidence in Scotti's estimate, but it appeared unconfirmed and was thus given very little weight.

Fig. 3 shows how our new quality classes compare with those from T00. A little more than half the comets (54) have kept the same quality class; the rest were assigned a new quality class, in particular moving from QC 4 to QC 3, which indicates that much of the improvement arises from comets, whose very uncertain estimated magnitudes in T00 can now be constrained within ±1 mag. We have fewer comets in the worst QC in the present version of the catalog.

Fig. 4 shows a comparison of the absolute nuclear magnitudes based on the analysis of all the available data and those estimated with the peer-reviewed data alone. For comets with QC $\leqslant$ 3 in both data sets (filled circles) we find a good agreement; since, as we mention above, we generally give a very high weight to the peer-reviewed data. Nevertheless there are a few cases where the peer-reviewed data points towards a brighter magnitude than the complete data set (e.g., 48P, Figs. 1c and 1d). There are many cases where the inclusion of the non-reviewed data allowed us to improve the quality class (upward triangles); in those cases the nuclear magnitudes based on the complete data are fainter than those based on the peer-reviewed data. The downward triangle at $x = 19$, $y = 20.4$, corresponds to Comet 87P/Bus. For this comet, as in the cases of 76P/West–Kohoutek–Ikemura and 147P/Kushida–Muramatsu mentioned above, there are HST observations by Lamy et al. much fainter than the others; though in the case of 87P we take a mean be-
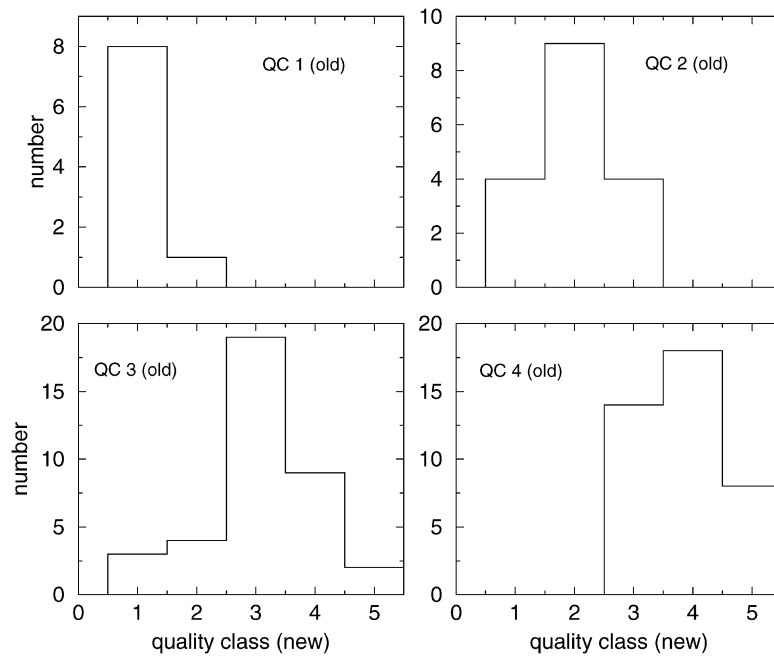
Fig. 3. Distributions of the new quality classes of comets, grouped into four panels according to the quality classes assigned in T00. Comets removed from the sample are classified as "QC 5."
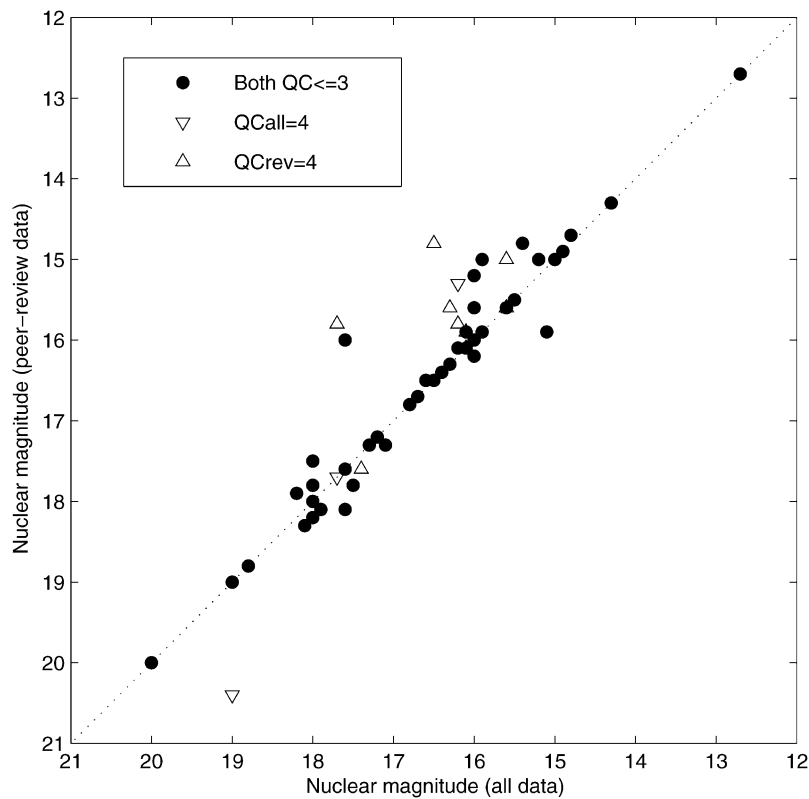

Fig. 4. The absolute nuclear magnitudes estimated with the complete data set are plotted versus those estimated with the peer-reviewed data only. Filled circles denote comets that have been classified as QC 1–3 in both sets; downward triangles are for comets classified as QC 4 in the complete data set and QC 1–3 in the peer-reviewed one, and upward triangles are for comets classified as QC 4 in the peer-reviewed data set and QC 1–3 in the complete one. A dotted line is drawn where both magnitudes are equal.

tween the faintest non-reviewed data and those of Lamy, leaving an uncertainty less than ±1.5 mag and classifying the object as QC 4.

Fig. 5 shows a plot of the absolute nuclear magnitudes as a function of the perihelion distances. As found in Fernández et al. (1999) (from here on F99), we note a depletion of small
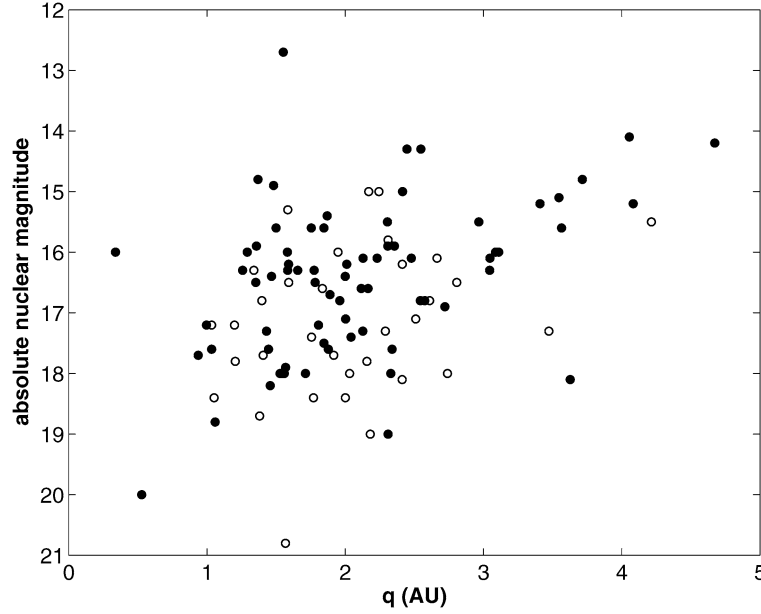
Fig. 5. Absolute nuclear magnitudes versus perihelion distances for the sample of JF comets shown in Table 1. Filled circles are for comets of quality classes 1 to 3. Open circles are for comets of quality class 4.

comets ($H_N \gtrsim 16.5$) for $q \gtrsim 2.5$ AU which is an indication of an observational bias against the discovery or the determination of nuclear magnitudes of small comets with large perihelion distances.

4. The cumulative luminosity function

F99 studied the cumulative luminosity function (CLF) of the sample of JF comets with $q < 2$ AU, finding that it could be well fitted by a linear relation up to $H_N \sim 16$, namely,

$$\log\left[N_H(< H_N)\right] = C + \gamma H_N, \qquad (2)$$

where the slope was found to be $\gamma = 0.53 \pm 0.05$, and C is a constant.

As mentioned above, since we are looking for the CLF of the entire population and not just from the biased observed one, we shall attempt to reduce the selection effects by considering, as we already did in F99, the sub-sample of JF comets with $q < 2$ or 2.5 AU for which we may presume the degree of completeness is higher than for more distant JF comets down to a lower size range. This effect can be seen in Fig. 6 where we plot the separate differential luminosity functions of comets with $q < 2.5$ AU and with $q > 2.5$ AU. The black bars corresponding to objects with $q < 2.5$ AU peak at $H_N \sim 18$, while those with $q > 2.5$ AU do so at $H_N \sim 16$. The most plausible way to explain this discrepancy is a selection effect that favors the discovery of comets when they are close to the Earth. In particular, the smallest comets may be too faint at large perihelion distances.

We have revised the CLF with our updated data sets and the new plots are shown in Fig. 7 for comets with QC between 1 and 3 and two different cutting q-values: $q < 2.5$ AU and $q < 2$ AU. We obtain a good fit up to a magnitude $H_N \sim 16.7$. For $H_N \gtrsim 16.7$ the observed distribution increasingly falls be-

low the linear relation, suggesting an increasing degree of incompleteness. The number of JF comets with $q < 2$ AU and $H_N \lesssim 16.7$ is 21, so our sample has slightly increased with respect to that used by F99 (18 comets). Furthermore, we extend the sample to comets with $q < 2.5$ AU since we see that we have acquired a better degree of completeness up to this limiting perihelion distance. The sample of comets with $q < 2.5$ AU and $H_N \lesssim 16.7$ is 32. Combining the information using these two cutting q-values gives us more confidence in the results.

The method to fit the data in the logarithmic scale deserves some comments. We try to fit the linear part of the curve for magnitudes in the region of completeness. We then characterize the goodness of the fit by computing the RMS of the *chi-square fitting* (i.e., RMS $= \sqrt{(\chi^2/(N-2))}$, where N is the number of points). First, we note that the plot contains 28P/Neujmin 1 which, with a magnitude $H_N = 12.7$, appears quite detached from the rest of the population. We have removed it from our derivation of the CLF, since it has a huge statistical weight which is not intrinsic, but arises from its radius being about three times greater than that for the second largest comet. Its inclusion would increase the RMS in all the fits and introduce undue distortions to our fitted curves. We thus start from the second largest comet of the population. Second, one has to define a lower size limit where the degree of incompleteness becomes too high. This is generally done by identifying a turn-off point with respect to the expected linear behavior. This definition may be very subjective, and we therefore introduce an objective criterion to make the choice. We consider a set of possible locations of the turn-off points and we compute the RMS obtained for all these locations. We select the fit with the lowest RMS. Thirdly, a simple regression line through the available data points for a given range of H_N-values, due to the logarithmic scale of the plot, would give very high weight to the clustering of data at the lower size range. We thus decided to

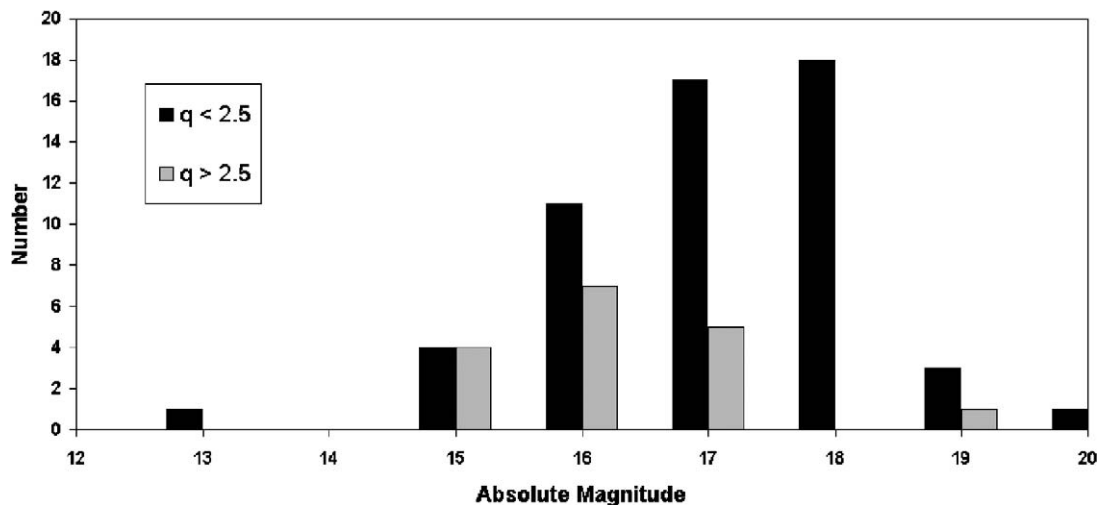Fig. 6. Histogram of absolute magnitudes for the samples of comets with $q < 2.5$ AU (black bars) and $q > 2.5$ AU (gray bars).
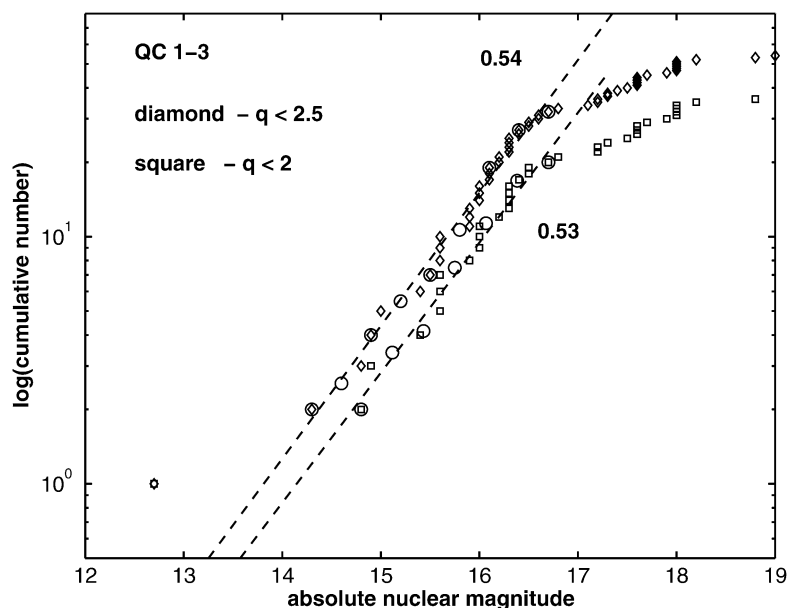

Fig. 7. The cumulative luminosity function (CLF) of the sample of JF comets with different cutting q-values. The upper curve with diamonds corresponds to JF comets with $q < 2.5$ AU, the lower one for those with $q < 2$ AU. A fit to the linear part for each curve is drawn with a dashed-line. The fitted points (as explained in the text) are the empty circles.

spread equally spaced values along the H_N axis and calculate the interpolated $\log N$ values. We fit a straight line to this set of points. These points are shown as empty circles in our plots. For the sample of comets with $q < 2.5$ AU we obtain a slope $\gamma = 0.54$ and for $q < 2$ AU the value is 0.53.

As a first check we made a similar plot including comets with QC = 4. Slightly larger values of the slope index are obtained (i.e., $\gamma \sim 0.61$). As a second check we made a similar plot with the absolute nuclear magnitudes based on the analysis of the peer-reviewed data set. We obtain a wide range for the slope index (i.e., $\gamma \sim 0.42$–0.59), due to the smaller sample.

From these results, we may conclude that the revised slope of the CLF is now $\gamma = 0.54 \pm 0.05$, where the error bar represents an estimated uncertainty based on variations of slope found for samples with different selection criteria or for differ-

ent parts of the curves. Hence, the uncertainty is not a mathematical estimate of the quality of the fit, but rather expresses the uncertainty arising from fitting a curve to a small data set. Our revised result for the slope γ is compatible with our previous estimate presented in F99.

5. The size distribution

The geometric albedos of cometary nuclei can be derived from two different approaches. One method uses observations of the thermal IR emission of the nucleus, which, together with a theoretical model for the temperature distribution in the surface layers, yields an estimate of the size of the nucleus. The other uses close-up imaging during a spacecraft flyby to derive the nuclear size. In both cases the visual albedo can then be obtained from photometry of the scattered sunlight in the visual

Table 3
Radii, shapes and V-band geometric albedos of well-studied Jupiter family comets, based on spacecraft imaging, thermal IR measurements or lightcurves and comparison with our own estimates

Comet	R_N (ours)	QC	Effec. R_N	p_V (%)	$b/a, c/a$	Source
2P/Encke	$1.95^{3.31}_{1.28}$	3	2.4 ± 0.3	4.6 ± 2.3	$0.56 \pm 0.03, -$	[a]
9P/Tempel	2.52	1	3.0 ± 0.1	4	$-, 0.64$	[b]
10P/Tempel	$4.02^{5.51}_{3.06}$	2	$5.3^{+0.2}_{-0.7}$	3.0 ± 1.0	$0.52 \pm 0.05, -$	[c]
19P/Borrelly	$2.56^{3.06}_{2.21}$	1	2.5 ± 0.1	2.9 ± 0.6	$0.39, -$	[d]
22P/Kopff	$1.78^{2.04}_{1.57}$	1	1.7 ± 0.2	4.2 ± 0.6	$0.66 \pm 0.05, -$	[e]
28P/Neujmin	$12.12^{15.6}_{9.92}$	1	10.0 ± 0.5	2.5 ± 0.8	$0.63 \pm 0.05, -$	[f]
31P/S-W	$3.03^{4.80}_{2.18}$	2	3.1 ± 1.0	$-$	$0.63 \pm 0.05, -$	[g]
48P/Johnson	$2.19^{3.48}_{1.58}$	2	2.6 ± 0.2	$-$	0.73	[h]
49P/Arend–Rigaux	$3.64^{4.46}_{3.06}$	1	4.6 ± 0.2	4.0 ± 1.0	$0.52 \pm 0.05, -$	[i]
81P/Wild	$2.21^{3.49}_{1.58}$	2	2.3 ± 0.1	3 ± 1.5	$0.73, 0.60$	[j]
143P/Kowal–Mrkos	$4.59^{7.78}_{3.00}$	3	5.7 ± 0.6	$-$	$0.61 \pm 0.04, -$	[k]

[a] Luu and Jewitt (1990), Fernández et al. (2000).
[b] A'Hearn et al. (2005).
[c] Jewitt and Luu (1989), Campins et al. (1995).
[d] Soderblom et al. (2002), Buratti et al. (2004).
[e] K.J. Meech quoted by Jewitt et al. (2003), Lamy et al. (2002).
[f] Jewitt and Meech (1988), Delahodde et al. (2001), Campins et al. (1987), Campins and Fernández (2002).
[g] Luu and Jewitt (1992).
[h] Jewitt and Sheppard (2004).
[i] Jewitt and Meech (1985), Millis et al. (1988), Campins et al. (1995).
[j] Brownlee et al. (2004) (the albedo was quoted as preliminary by the authors).
[k] Jewitt et al. (2003).

region. Unfortunately, the number of studied comets for any of the two approaches is still quite small.

A great problem with measuring the thermal emission is that the nucleus may be blended by surrounding dust, if the comet has substantial activity, and under such circumstances it may be impossible to identify the nuclear contribution to the detected radiation with certainty. This is likely to cause some bias of the observed sample, because the observations have a tendency to focus on comets known for their low activity, like 49P/Arend–Rigaux or 28P/Neujmin 1. Such comets are found among those with the largest nuclei, probably because smaller nuclei do not develop extensive mantling as easily, and thus the set of measured albedos may have an overrepresentation of large nuclei.

This circumstance calls for special care when deriving the size distribution from the CLF. We should use the knowledge of individual albedos, but in the absence of evidence to the contrary, we have to treat the unobserved majority of comets in full consistency with the values found for the observed minority. Otherwise we could face the risk of introducing an error into the slope of the size distribution, e.g., the slope could be flattened if we use a low albedo for the largest objects and assume a higher value for the smaller ones.

Table 3 lists the nuclear radii and albedos of well-studied Jupiter family comets, based on direct observations, and references to the sources of information. Note that the albedo error bars, as quoted from the literature, are always substantial and sometimes very large. We have recomputed the radii based on our derived nuclear magnitudes with the nominal value of the albedo for each individual object. Therefore, there are differences with the corresponding radii presented in Table 1, since those values where computed with the standard albedo of 0.04. The upper (lower) value to the right of the nominal radius is calculated with the nominal albedo minus (plus) the stated error and then multiplied by $1+ (1-)$ maximum relative error corresponding to the assigned quality class QC. The assigned quality class QC for each comet associated to the nuclear magnitude estimate is also given. The uncertainties in the radius associated to each quality class are presented in Section 3.

For 81P/Wild 2 our reference is the first paper with spacecraft results, where the analysis is still preliminary, and better estimates may become available later on. For 28P/Neujmin 1 we judge that the albedo may have an additional uncertainty, since our source is a recent review, and earlier original research papers gave widely differing results. The albedo value of 9P/Tempel 1 has been downward revised recently with the data from the Deep Impact mission (A'Hearn et al., 2005). The previous albedo estimate of $p_R = 0.072$ by Fernández et al. (2003) and our derived magnitude $H_N = 15.6$ would imply a comet smaller than 2 km in radius, but with the new value of $p_V = 0.04$ we obtain an estimated mean radius of 2.5 km, much closer to the value measured by Deep Impact of 3 ± 0.1 km.

From the CLF we can derive the cumulative size distribution (CSD) $N_R(R_N)$, bearing in mind that, according to Eq. (1) in T00:

$$\log\left(p_V \pi R_N^2\right) = 16.85 + 0.4(m_\odot - H_N), \qquad (3)$$

where R_N is expressed in kilometers. The apparent visual magnitude of the Sun is $m_\odot = -26.77$.
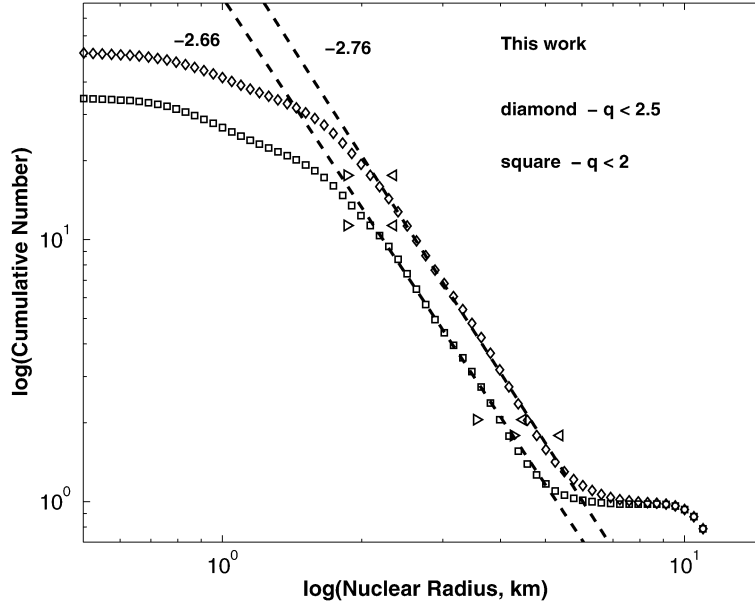
Fig. 8. The cumulative size distribution of the sample of JF comets with different cutting q-values. The CSD is constructed as the sum of the individual probability density functions for each comet assuming a normal albedo distribution (see text). We sampled the CSD at equally spaced values along the log R_N axis. The upper curve with diamonds corresponds to JF comets with $q < 2.5$ AU and the lower curve is for those with $q < 2$ AU. A fit to the linear part for each curve is drawn with a dashed-line. The fitted points are between the upper and lower triangular marks for each curve.

If we introduce this relation into Eq. (2) and assume a constant value of the albedo, we obtain

$$N_R(> R_N) \propto R_N^s, \qquad (4)$$

where $s = -5\gamma$. For the value of γ obtained in the previous section, we get $s = -2.7 \pm 0.15$.

As shown above, we are beginning to have reliable information about the albedos of some particular comets as well as a distribution of typical albedo values of JF comets. Let us now use this information to derive an improved relation between the CLF and the CSD, relaxing the assumption of a constant albedo.

For each individual comet we will assume a distribution of the albedo according to available information, i.e.:

- if a given comet has a reliable measurement of the albedo with a certain error bar (Table 3), we assume for this comet an albedo distribution with a Gaussian shape (within $\pm 2\sigma$), centered on the reported value and σ equal to the reported error;
- if we do not have any information about the albedo of the object, we assume an albedo distribution with a normal shape (within $\pm 2\sigma$), centered at the mean and standard deviation of the values presented in Table 3.

From Eq. (3), we derive the relation between p_V and log R_N as

$$p_V = \frac{10^C}{\pi} \exp(-2\ln 10 \log R_N), \qquad (5)$$

where $C = 16.85 + 0.4(m_\odot - H_N)$.

Let us consider two variables x and y with probability density functions (PDF) $p(x)$ and $p(y)$, respectively. According to

the transformation law of probabilities we have

$$p(y) = \left| \frac{\delta x}{\delta y} \right| p(x). \qquad (6)$$

The relation between the PDFs of p_V and log R_N then becomes

$$p(\log R_N) = 2\ln 10 \, p_V \, p(p_V). \qquad (7)$$

For a given value of H_N and a given $p_i(p_V)$ for each individual comet (identified by index i), by substituting Eq. (5) into Eq. (7), we obtain the individual probability distribution of log R_N. Adding the individual $p_i(\log R_N)$, we obtain the differential size distribution (in terms of log R_N) for the whole sample, from which we can easily compute the CSD. We have tested other shapes for the albedo PDF rather than the normal one (e.g., a triangular shape); the results are not sensitive to the assumed shape of the PDF.

We have revised the CSD with our updated catalog of nuclear magnitudes and the assumed albedo distribution. In Fig. 8 we present the CSD with different cutting q-values for comets with QC between 1 and 3. In order to compute the slope of the linear fit in the log–log plot we sample the CSD at equally spaced values along the log R_N axis and compute the corresponding log N values. We fit a straight line to this set of points. In order to define the linear part of the curve, we apply a technique similar to the one explained above: we choose the fit with the lowest RMS among different choices of the turn-off point. We obtain a mean value between the two curves (with different limiting perihelion distance) of $s = -2.69$, quite similar to the value obtained by assuming a fixed value of the albedo. We have thus shown that by treating the albedo distribution in a consistent way according to the present uncertainties, we obtain similar results either by assuming a fixed value for the albedo or using a distribution of albedos.

We conclude that a value for the CSD index of $s = -2.7 \pm 0.3$ results from a careful comparison of the different methods and selection criteria.

6. Comparison with other CSDs

The three research groups mentioned in Section 3 have also produced their own compilations of size estimates using different selection criteria. In Fig. 9 we compare the three estimates with the values presented in Table 1. In spite of the differences in the selection criteria and the criticism by other authors (see e.g., Me04, La05, and Weissman and Lowry, 2003) about the heterogeneity of our data set, we notice a general agreement among the different estimates and a reasonable amount of scatter around the $y = x$ line. Detailed considerations of the major discrepancies are presented below.

Neslušan (2003) (hereafter Ne03) has also produced a compilation of size estimates of short- and long-period comets. Since a large proportion of his estimates (65 out of 105) are taken from our previous catalog (T00), we have not made any specific comparison with his data.

Table 3 compares our estimated radii with a few JF comets for which it has been possible to determine their radii and shapes (in general given as the ratio b/a of the semi-axes a and b of the body, assumed to be a triaxial ellipsoid whose minor axes $b = c$), either by close-range direct imaging, by ground-based thermal-IR observations, or determining the lightcurves, when they are inactive or the signal from the nucleus can be separated from the coma. As we can see in the table, the agreement between the effective radii and our estimated radii can be considered good; for 7 out of the 11 listed comets the differ-
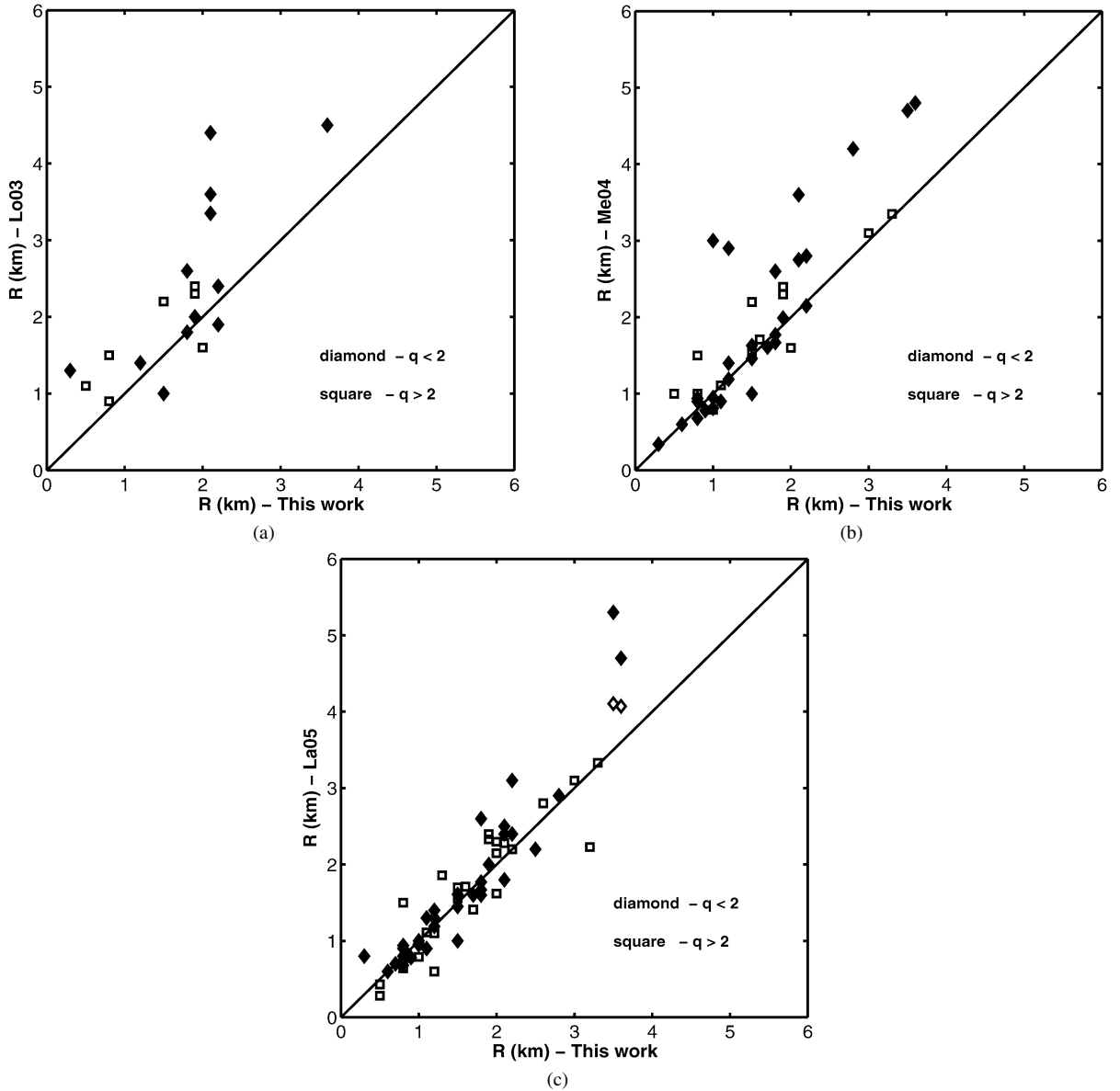

Fig. 9. Plot of our estimated nuclear radii from Table 1 versus the other data sets: (a) Lowry et al. (2003) (Lo03), (b) Meech et al. (2004) (Me04), (c) Lamy et al. (2005) (La05). Filled diamonds represent comets with $q < 2$ AU, while empty circles are for comets with $q > 2$ AU. In plot (c) we include two empty diamonds that correspond to Comets 10P/Tempel 2 and 49P/Arend–Rigaux, corrected to a common albedo value (see text in Section 3).

Table 4
Comparison of the estimates of cumulative size distribution exponent (s) as published by different authors

Paper	s	q-range	Size range (km)
This work	−2.76	$q < 2.5$ AU	1.7–5.5
This work	−2.66	$q < 2$ AU	1.7–4.5
Fernández et al. (1999)	−2.65	$q < 2$ AU	2.1–3.3
Lamy et al. (2005) (La05)	−1.66	All q	>0.9
	−2.50	All q	1.5–5
Lowry et al. (2003) (Lo03)	−1.6	All q	>1.7
Weissman and Lowry (2003) (WL03)	−1.59	All q	>1.4
Neslušan (2003) (Ne03)	−3.04	All q	>0.8
Meech et al. (2004) (Me04)	−1.45	All q	1–10
	−1.91	All q	2–5

ences are within 20%. Interestingly, larger discrepancies tend to occur for comets that are more elongated. Part of the reason might be that our estimated R_N for these two comets were determined relying principally on observations taken around the minimum of the lightcurve.

The four groups that produced nuclear magnitude catalogs have also analyzed their data sets to estimate the size distribution exponent. In addition, Weissman and Lowry (2003) (hereafter WL03) have produced a compilation of nuclear size estimates, though they have not published the data for the individual comets in tabular form. They just showed the plot of the CSD and an estimate of the exponent. In Table 4 we present the estimates of the CSD exponent made by the different groups. All the other groups, with the exception of Neslušan (2003) have claimed values of the exponent on the order of −1.4 to −1.7, much lower, in absolute terms, than our value of −2.7. This is a striking situation, since some of the compilations rely on the other (e.g., La04 is a compilation of their own data plus Lo03 plus T00). How could people working with similar data sets obtain so different results? We will review the different estimates in turn, comparing them with ours and analyzing the sources of the discrepancies.

Lamy et al.'s (2005) distribution is presented in their Fig. 4a which plots two curves: the lower one for what they call "ecliptic" comets (similar definition to Jupiter family comets) and the upper one for "ecliptic" comets plus "cometary" near-Earth asteroids (NEAs)—asteroids suspected of being inactive comets. A first criticism is the criteria chosen by the authors to select the NEA candidates. They include asteroids with T much greater than 3 and $T < 2$ in the list of candidates for "ecliptic" comets. It is almost dynamically impossible to transform an "ecliptic" comet into an object with $T = 4.5$ like 3200 Phaethon. Furthermore, there are clear indications that some of these objects could well be *bona fide* asteroids, either from the dynamical point of view (Fernández et al., 2002) or from physical observations of these objects (Binzel et al., 2004; Licandro et al., 2005), and thus a different class of bodies than JF comets. It is also unclear how complete is the sample of "cometary" NEAs down to a size of a few kilometers, bearing in mind that many of these objects were discovered in recent years. The authors are thus adding a spurious and possibly incomplete sample in a critical part of the size distribution curve. A visual inspection of the two curves shows that they have a different slope. This is due to the fact that

many NEAs are included in the size range 3–10 km. Due to the considerations presented above, we leave aside their analysis of the size distribution of comets plus NEAs. If the analysis is concentrated on the "ecliptic" comets alone, the authors conclude: "*In order to fit a power-law, we introduce a cut-off at $r_c = 0.9$ km and find $s = -1.87 \pm 0.02$, a value rather insensitive to the exact choice of r_c. As illustrated in Fig. 4a, the fit is very poor and the slope is entirely controlled by a single large nucleus, that of 28P/Neujmin 1. There is an intermediate part of the cumulative size distribution defined by $1.5 < r_N < 5$ km, which exhibits a steeper slope, namely $q_s = -2.50 \pm 0.03$.*"

Looking at their Fig. 4a, we see that the fit with a slope of −1.87 is done including sizes smaller than the turn-off point of the CSD, and this is bound to seriously flatten the slope. But the value obtained in the linear part of the CSD curve agrees with our estimate. Nevertheless, as we mentioned above, by considering the entire sample of observed JF comets, one mixes populations with different completion factors. The differential size distribution for comets with $q < 2$ AU and for those with $q > 2$ AU for the La05 data set is shown in Fig. 10. As in our data set, the differential distribution for comets with larger q has a peak at higher values of the radius as compared to the distribution of comets with lower q.

Therefore, as we have already done with our data, we analyze the La05 CSD with different cutting q-values (Fig. 11). For consistency, we have converted all the size estimates of La05 to a uniform albedo of $p_V = 0.04$. There are a few large and inactive comets that have albedo estimates lower than this value (i.e., 10P/Tempel 2 and 49P/Arend–Rigaux). But, as the authors assumed a standard albedo of 0.04 for the rest of the comets, the use of a lower p_V for the largest comets would introduce a strong bias in a critical part of the CSD. From their data we obtain an exponent of $s = -2.15$ in the range $1.6 < R_N < 4$ km for comets with $q < 2$ AU, but a much larger value in absolute terms for the complete sample ($s = -2.91$). The value for $q < 2$ AU is smaller (in absolute terms) than our value, but still larger than the value of Table 4 claimed by the authors. As clearly seen from the plot, if we go beyond $R_N \sim 1.6$ in both curves the goodness of the fits deteriorates since the curves start to depart strongly from the linear behavior.

The discrepancy between our results and theirs for comets with $q < 2$ AU, comes from an important deviation of most size estimates for $R_N > 2$ km, as shown in Fig. 9c. If we just
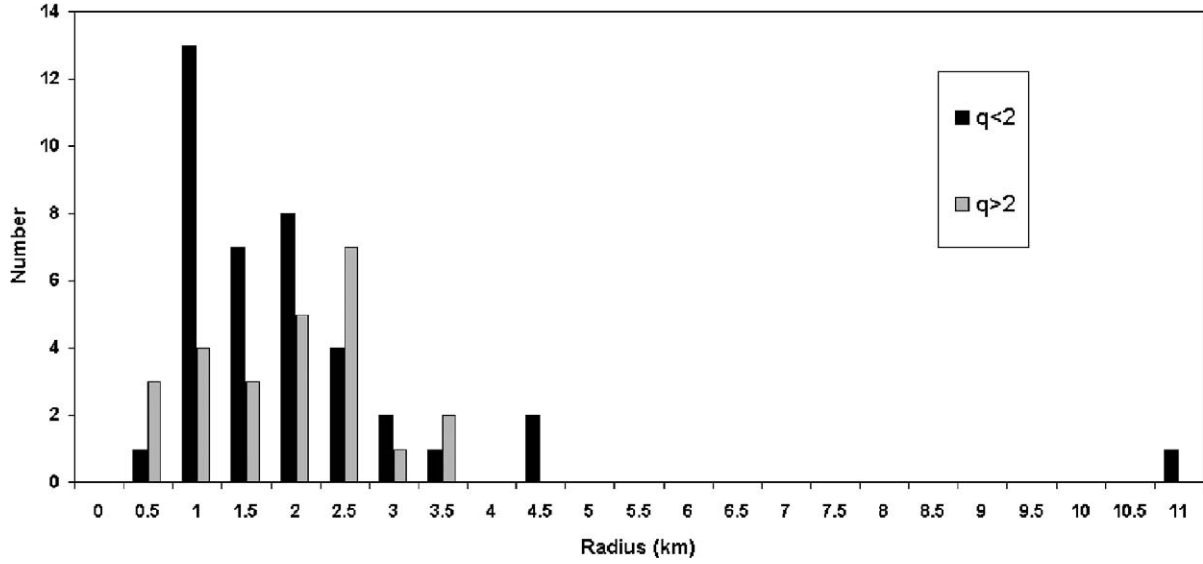
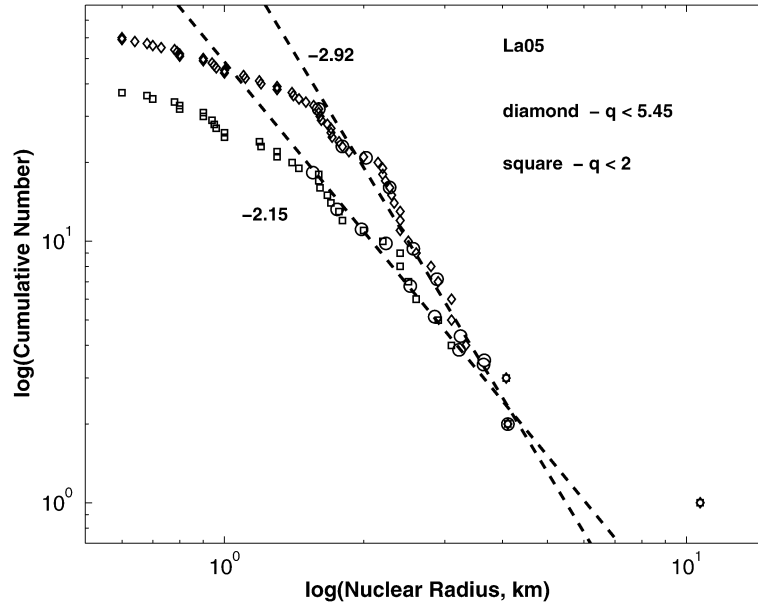Fig. 10. Histogram of radius for the samples of comets with $q < 2$ AU (black bars) and $q > 2$ AU (gray bars) for La05.

Fig. 11. The cumulative size distribution of the sample of JF comets with different cutting q-values for La05. The upper curve with diamonds corresponds to all the JF comets ($q < Q_J = 5.45$ AU). The lower curve is for comets with $q < 2$ AU. A fit to the linear part for each curve is drawn with a dashed-line. The fitted points (as explained in the text) are the empty circles.

look at the objects with $q < 2$ AU, there is a much larger discrepancy between the La05 estimates and ours for comets with $R_N > 2$ km than for those with $R_N < 2$ km. For comets with $q < 2$ AU (filled diamonds in the plot) their values are generally larger than ours in the right part of the plot. The objects showing the largest discrepancies are: 49P/Arend–Rigaux, 10P/Tempel 2, 9P/Tempel 1, 67P/Churyumov–Gerasimenko, and 7P/Pons–Winnecke. In all cases, there are observations in our catalog that contradict La05's estimates with magnitudes much fainter than their assumed value. The effect of this deviation in the CSD is to flatten their curve leading to a lower exponent. The most striking discrepancies occur for the two largest plotted comets: 10P/Tempel 2 and 49P/Arend–Rigaux (28P/Neujmin 1 is out of the scale), even though for the CSD curve we use the val-

ues corrected to a uniform albedo that are shown as two empty diamonds in the plot.

The analysis of the CLF by Lowry et al. (2003) (Lo03) is based on their own set of observations. The CLF is presented in their Fig. 5b both for a sample of active plus unresolved comets, and for the unresolved comets alone. The CLF for active and unresolved (possibly inactive) comets is of no use for the analysis of the CSD, because there is no reliable way to relate the sizes to the total magnitudes. Furthermore, the inclusion of several objects brighter than their real nuclear magnitude due to the coma contamination, would flatten the CLF. Therefore we will make no further comments about the combined CLF. Regarding the sample of unresolved comets, we first note that their total sample is very limited; it contains 19 comets, 12 with $q < 2$ AU

and 7 with $q > 2$ AU. This is a small sample if we want to make a separate analysis with different q-limits. As shown in Fig. 9a, they have some estimates quite different from ours (in fact, comparing with the estimates of any other group, the Lo03 data shows important differences). In particular, the brightest comet in their sample is 2P/Encke with a nuclear V-magnitude $H_N = 14.1$ (a radius of 4.4 km), while all the other groups list in their compilations much lower estimates for the radius of this comet of 2–2.4 km ($H_N \sim 16$). Recently Fernández et al. (2003) presented a set of observations of this object when it was close to aphelion. Their distance reduced magnitudes are brighter than our derived nuclear magnitudes and close to the Lo03 value, but they suspect that their observations were contaminated by an unresolved coma. The true nuclear magnitude of 2P/Encke is still an open question; hence our assumption of QC 3 is reasonable. The nuclear magnitude of 2P is a very critical value in Lo03's CLF, since it is the second largest object. Changing its value or removing it from the sample would strongly affect the slope. But the main problem in their analysis is the small size of the sample that prevents us to make a classification in separate q-groups and it makes any resulting CSD slope vulnerable to uncertainties in individual data points.

The comparison with the size distribution of WL03 is more difficult, since they have not published the full version of their catalog yet. This catalog is based on "reduced and calibrated measurements by professional astronomers," including their own data set (which was published in a series of papers compiled in Lowry et al., 2003). As shown in Fig. 9a, Lowry et al.'s estimates of nuclear magnitudes tend to be much brighter than La05 or our estimates. Depending on the weight that they gave to their own data, this deviation might introduce an important difference in the size distribution at larger radii. But the most critical aspect of the WL03 analysis may be their definition of Jupiter family comets. This problem has already been noticed by La05. Though WL03 quote Levison's (1996) classification for Jupiter family and Halley-type comets, which uses T as discriminant, they in fact use the old criterion of the orbital period to distinguish between the two populations (period shorter or longer than 20 years). This inconsistency led them to include some (at least two) objects in their sample that are not present either in La05 or in our sample.

Their largest and third largest objects are 29P/Schwassmann–Wachmann 1 with a radius $R_N \approx 15.4$ km and 8P/Tuttle with $R_N \approx 7.3$ km (Lowry, private communication). 8P/Tuttle is not a Jupiter family comet with any of the commonly accepted definitions since it has $T = 1.68$, much lower than 2. 29P/Schwassmann–Wachmann 1 is an unusual comet whose orbit lies completely outside the orbit of Jupiter ($q = 5.7$ AU). With Levison's definition it would be a borderline case, but with $T = 2.98$ and $a > a_J$ it should be considered almost as a Chiron-type object. With our definitions introduced in Section 2, it should be classified as a centaur, just like 95P/Chiron. 29P as well as 95P belong to a population of objects where observations are very incomplete, and the inclusion of the former in the size distribution of Jupiter family comets introduces an important bias in the large size range. As we did not have access to the raw data, we digitized Fig. 1 of WL03 and recreated

the data table. Taking away the two spurious objects, we made a new plot of their size distribution (Fig. 12). Unfortunately, we are not able to make the distinction between objects with q higher or lower than 2 AU. We see again that the largest object in their sample (at $R \sim 9.7$ km) is quite detached from the linear part of the curve. As before, we start the fit from the second largest point. This assumption is also based on the analysis of the goodness of the fit. The best RMS computed starting in the first point is much larger than the one computed from the second point. In the range $2.2 < R_N < 5.9$ km and for the whole population of Jupiter family comets we obtain a slope of -2.38, close to our estimate.

Neslušan (2003) (Ne03) obtained a slope index of -3.04 from his sample of short-period comets. There is no wonder that he obtained a value similar to our previous estimate of -2.65 (F99), since a large fraction of his data set (65 out of 105) was taken from our previous version of the catalog (T00). Nevertheless, since he included a few Halley-type comets and 40 radius estimates different from our previous values, we have reanalyzed his data set like we did with the other groups. Neslušan includes into his table of new size estimates a very large object: the lost Comet D/1960S1 (van Houten) with a radius of 14.8 km. The estimate is based on a single tabular listing by Svoreň (1987). As can be seen in Ne03's Table 1, several of the sizes derived from Svoreň (1987) are much larger than the ones reported by other authors. We deem the D/1960 S1 estimate to be a very doubtful value, so we have removed it from our analysis. Neslušan's way of computing the size index was slightly different from the others, since he fitted a power-law to the linear plot of R vs cumulative number, rather than a straight line to the log–log plot. We apply our usual way of computing the size index to his data set, thus obtaining a value of -2.67. Let us correct an error in Ne03's Discussion section, where he says: "*The slope index s between ≈2.7 and ≈3 for SP comets appears to be in contradiction with s = 0.88 found by Fernández et al. (1990) for the Jupiter family-comet radii….*" The value 0.88 refers to our estimate of the mass index, rather than the size index. The mass index is (assuming equal density among the comets) 1/3 of the size index. Using the correct value of -2.65, Neslušan would have found both estimates to be much closer.

The sample of comets contained in Meech et al. (2004) (Me04) includes JF comets as well as Halley-type and long-period ones. This is a very heterogeneous sample with important selection effects, for which bias corrections should be applied in different ways to each population. From their compilation they obtained a CSD exponent $s = -1.45 \pm 0.05$ for the range $1 < R_N < 10$ km, and $s = -1.91 \pm 0.06$ for the range $2 < R_N < 5$ km. Let us now use their data and select only the JF comets. The CSD for their sample of JFCs is presented in Fig. 13 for the same two cutting q-values as in Fig. 11. We obtain a slope for the linear part of the distribution that is higher than the value claimed by Me04 and closer to our own estimates.

Me04 made an attempt to obtain the debiased CSD by applying a complex model for the different selection effects. Their model has many free parameters. In particular the authors have
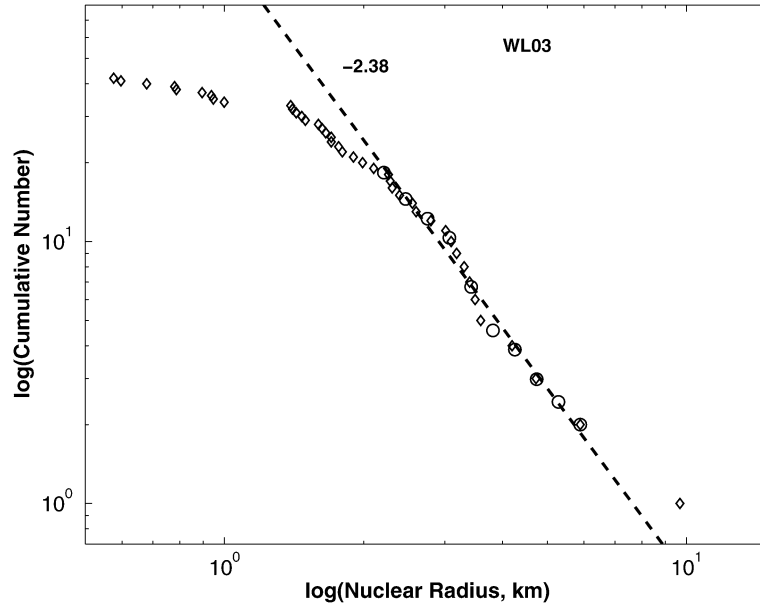
Fig. 12. The cumulative size distribution for the sample of comets of WL03 after taking away the two comets that do not belong to the JF (see text).
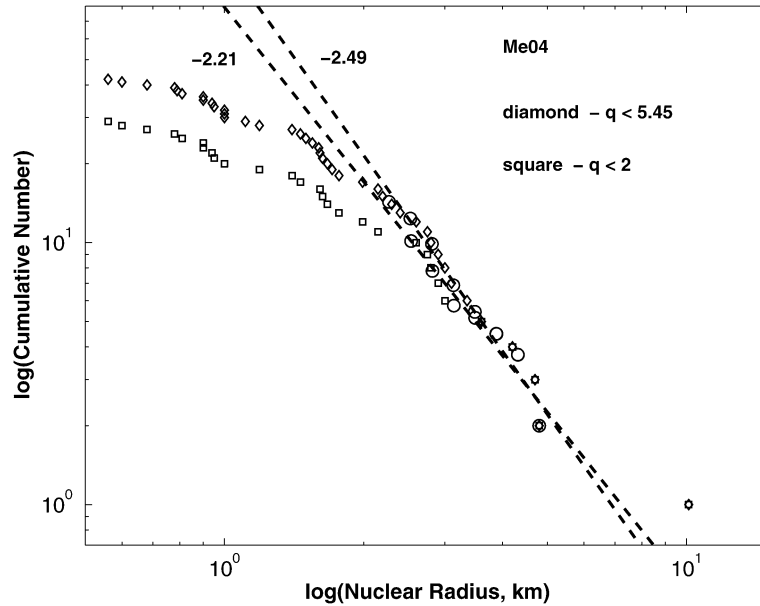

Fig. 13. Similar to Fig. 11 but for Me04's data.

to assume a CSD for the total population and fit the outcome of that model to the observed distribution. After experimenting with different sets of parameters, they conclude that the best fit corresponds to a CSD with an exponent of -2.5 (-3.5 for the differential size distribution) and a truncation of the distribution at a small nuclear radius. But rather than concluding that their derived CSD exponent for the entire cometary population is similar to the one obtained by F99, Meech et al. focused on their raw data and argued the opposite, i.e., that our value is in disagreement with those of the other investigators. Doing this, they overlooked the fact that, while all the other estimates are based on the total observed sample of cometary nuclear magnitudes, affected by different selection effects, we concentrated our analysis in a sub-sample that corresponds to a more ho-

mogeneous population in the dynamical sense (the JFCs) with a high degree of completeness (comets with $q < 2$–2.5 AU); therefore we do not have to debias the sample in order to obtain an estimate of the CSD exponent of the entire population. This is the reason of the general agreement between the results of their debiased model and our estimate.

In Fig. 14a we plot the CSDs of La05, Me04 and ours for comets with $q < 2$ AU, and in Fig. 14b we plot the CSDs of the four previous data sets and from WL03 for all the observed JFCs, in order to show that the application of a common criterion to select the sample leads to similar CSDs. Lines of different slopes are shown at the right side of the plot. It is clear from both plots that the slope of 1.5 is not compatible with the linear part of the curves; rather, slope values between
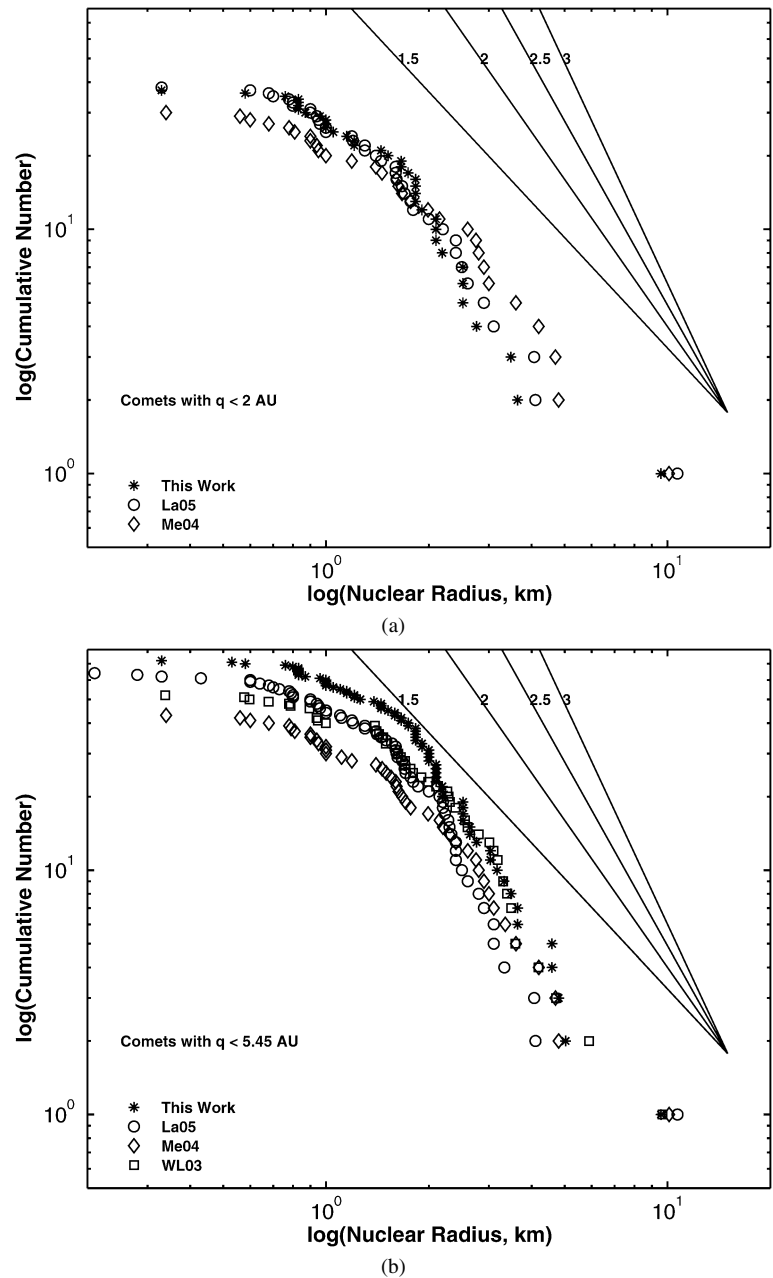
Fig. 14. Comparison between our current cumulative size distribution and the ones from La05, Me04, and WL03. (a) Comets with $q < 2$ AU; (b) comets with $q < 5.45$ AU. As a check we plot different slopes from 1.5 to 3.

Table 5
Comparison of the revaluated estimates of cumulative size distribution exponent (s)

Data set from	s	q-range	Size range (km)
Lamy et al. (2005) (La05)[a]	−2.91	All q	1.6–4.1
	−2.15	$q < 2$ AU	1.6–4.1
Weissman and Lowry (2003) (WL03)[b]	−2.38	All q	2.2–5.9
Meech et al. (2004) (Me04)[b]	−2.49	All q	2.3–4.8
	−2.21	$q < 2$ AU	2.5–4.8

[a] For consistency, we have converted all the size estimates of La05 to a uniform albedo of $p_V = 0.04$.
[b] Only JFCs as defined in Section 2 are included.

2 and 3 are needed. In Table 5 we present a compilation of the revaluated value of the exponent s for the different authors' data sets as discussed above. We thus conclude that with

a common definition of the Jupiter family population according to commonly accepted criteria and a detailed analysis of the data, we can reconcile the differences in the estimates of

the exponents of the CSD to a value consistent with our result.

We can compare our exponent s of the cumulative size distribution with the exponents found for other classes of bodies. For instance, Rabinowitz (1993) found $s = -2$ for NEAs, i.e., shallower than ours, while Jedicke and Metcalfe (1998) found a flatter distribution ($s \sim -1.5$) for small asteroids ($<$ a few km diameter) from the Spacewatch survey. Jewitt et al. (2000) found $s = -2.0 \pm 0.3$ for jovian trojans. A more relevant comparison is with the putative source of JF comets, i.e., the trans-neptunian region. Gladman et al. (2001) revised the CLF of TNOs by combining the results of several surveys. They obtained a slope $\gamma = 0.69 \pm 0.06$, which corresponds to $s = -3.45 \pm 0.3$ down to objects larger than ~ 50 km in radius. This exponent of the CSD is larger (in absolute terms) than our value for JFCs, but it corresponds to a different size range. From analytical and collisional models for the evolution of the size distribution of icy bodies in the Edgeworth–Kuiper belt, it is expected that the CSD will flatten out at small sizes. Indeed, Kenyon and Bromley (2004) found in their models power-law distributions with an index $s = -2.5$ to -3 for small bodies with radii 0.1–1 km, and an index $s \simeq -3.5$ for larger bodies ($R \gtrsim 10$–100 km). Hence, their index for small bodies—extrapolated to the size range of the bulk of the Jupiter family population—is close to our value. Recently, Bernstein et al. (2004) performed a deep TNO survey with the HST trying to extend our knowledge of the CLF in the faint-end. Based on the scarcity of discovered objects and combining their data with the other surveys, they fit the CLF with a double power-law. In the faint-end they obtained slopes γ between -0.5 and 0.4 for the different dynamical groups in the TNO region (note the almost unphysical negative values for γ), which corresponds to a range in the exponent s of CSD between $+2.5$ and -2. Although, this new deep survey is an improvement respect to previous attempts to reach the faint-end of the TNO's CLF, it seems that we should expect a wider sky-coverage down to magnitudes fainter than $R \sim 27$ before we can compare the observed CLF in the TNO region with the corresponding one of the JFC.

7. The fraction of active surface area

The determination of the radius of a cometary nucleus allows us to compute the fraction of active surface area, if we also know the gas production rate at a given heliocentric distance close to the Sun. Let us thus consider a cometary nucleus of radius R_N. When it is close to the Sun (say, $r \lesssim 3$ AU), the gas production rate is controlled by the sublimation of water. Let Z be the outgassing flux per unit area of exposed water ice (averaged around the surface of a spherical nucleus), which will be a function of the heliocentric distance r. The total water production rate (molecules per second) is given by

$$Q_{H_2O} = 4\pi R_N^2 f Z, \qquad (8)$$

where f is the fraction of active surface area of the comet nucleus.

We have computed values of $Z = Z(r)$ by means of the surface energy balance equation for a hypothetical comet nucleus
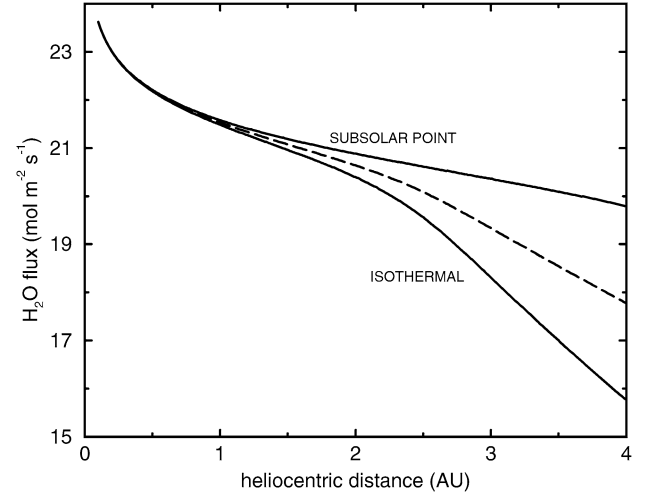

Fig. 15. Theoretical curves of the gas production rate per unit area of water ice as a function of the heliocentric distance for a body with $A_V = 0.04$ and $A_{IR} = 0$. Two extreme cases are considered: one isothermal and one ("subsolar point") with a hemisphere constantly oriented toward the Sun (based on the energy balance at the subsolar point). The average of these extremes is represented by the dashed curve.

of (visual) Bond albedo $A_V = 0.04$ and thermal infrared albedo $A_{IR} = 0$, and for two extreme cases: (a) an isothermal nucleus, and (b) a nucleus with a sunward-oriented spin axis. We assume that water ice is the only sublimating material. The results are insensitive to A_V, provided $A_V \ll 1$. Note that for the two particular cases (a) and (b) under consideration, heat conduction plays no role in the energy balance, and the water flux is only a function of the heliocentric distance. The two extreme curves of models (a) and (b) and an average curve are shown in Fig. 15. There is not much difference between the two extreme cases out to $r \sim 2$ AU, so we will simply adopt the average curve for our calculations. However, the solutions start to diverge quickly for larger r, so we only consider H_2O production rates observed at $r < 2$ AU.

Gutiérrez et al. (2003) have analyzed the gas production rates of slowly rotating irregular model bodies with different activity patterns on their surfaces. They compared the results from these models with those obtained from the simpler spherical model under average insolation. They find that the fast rotation and subsolar point approximations generally yield large over- and under-estimates, respectively, of the active area fraction, but that acceptable relative errors ($<100\%$) are obtained at small heliocentric distances ($r \lesssim 2$ AU). Therefore, Gutiérrez et al.'s conclusion lends additional support to the use of our simple model of a spherical nucleus, as long as we constrain its applicability to distances $r < 2$ AU.

The water production rate Q_{H_2O} can be derived from visual, radio and UV observations of hydrogen, OH and other radicals such as CN, C_2, and C_3. The water production rates of some JF comets and the heliocentric distances at which they were measured from narrow-band photometric and spectrophotometric observations of OH and $O(^1D)$ in the visible region are shown in Table 6. We mainly used the A'Hearn et al. (1995) results to maintain internal coherence. Their data constitute the largest uniform database available on comet water production

Table 6
Measured gas production rates and fractions of active surface area

Comet	$\log Q_{H_2O}(r)$	r (AU)	Ref.	f
2P/Encke	27.87, 28.30, 28.11	0.71, 0.33, 0.50	AH, Cr, Ma	0.02, 0.01, 0.01
4P/Faye	27.70	1.78	AH	0.18
6P/d'Arrest	27.51, 27.48	1.41, 1.40	AH, Cr	0.07, 0.06
7P/Pons–Winnecke	27.51	1.42	FH	0.06
9P/Tempel	28.09	1.41	AH	0.11
10P/Tempel	27.12	1.78	AH	0.01
16P/Brooks	27.01	1.78	AH	0.05
19P/Borrelly	28.31, 28.48	1.41, 1.43	AH, Cr	0.24, 0.37
21P/Giacobini–Zinner	28.55, 28.78, 28.71	1.12, 1.04, 1.05	AH, Cr, Cr	1.09, 1.54, 1.34
22P/Kopff	28.37, 28.46	1.78, 1.68	AH, Cr	0.82, 0.83
24P/Schaumasse	28.46, 28.00	1.21, 1.28	FH, Cr	1.29, 0.52
26P/Grigg–Skjellerup	26.67	1.12	AH	0.01
28P/Neujmin	27.20	1.41	AH	0.001
43P/Wolf–Harrington	27.62	1.78	AH	0.11
45P/Honda–Mrkos–Pajdušáková	26.88, 28.18	1.12, 0.55	AH, Cr	0.21, 0.85
46P/Wirtanen	27.97, <28.18	1.12, 1.12	AH, Cr	0.86
49P/Arend–Rigaux	27.23	1.41	AH	0.007
64P/Swift–Gehrels	27.99	1.53	NS	0.21
67P/Churyumov–Gerasimenko	27.59, 27.95	1.41, 1.35	AH, Cr	0.05, 0.10
68P/Klemola	26.95	1.78	AH	0.02
69P/Taylor	27.19	1.78	AH	0.04
73P/Schwassmann–Wachmann	27.62, 29.35[a]	1.44, 0.98	FH, Cr	0.27, 5.46[a]
81P/Wild	28.11, 27.90	1.58, 1.74	Ma, Cr	0.28, 0.23
97P/Metcalf–Brewington	28.13	1.78	AH	0.75
98P/Takamizawa	28.35	1.78	AH	0.31
103P/Hartley	28.35	1.12	AH	0.47
108P/Ciffréo	26.69	1.78	AH	0.08

Notes. AH: A'Hearn et al. (1995); Cr: Crovisier et al. (2002); Ma: Mäkinen et al. (2001); FH: Fink and Hicks (1996); NS: Newburn and Spinrad (1989).

[a] Observed after the comet split.

rates. For a few comets that have no data in A'Hearn et al. (1995), we took some spectrophotometric results from Fink and Hicks (1996) and Newburn and Spinrad (1989), some Lyman-α observations from Mäkinen et al. (2001), and some radio observations of the OH 18-cm line from Crovisier et al. (2002). As mentioned above, we only consider observations at $r < 2$ AU, for which the outgassing flux Z does not depend strongly on the model adopted.

If we take the central value of the assumed albedo distribution (usually, $p_V = 0.04$), and use the corresponding nuclear radii, we can compute the fractions of active surface area for the sample of JF comets, for which water production rates have been observed at $r < 2$ AU. Results are shown in Fig. 16 and Table 6. For those objects with more than one estimate of the water production, we plot the different values connected with a dotted line. Almost all the studied comets give consistent results for f within the range $(0, 1)$. In particular, 15 out of the 27 comets of the sample have fractions $f < 0.2$ (13 out of 21 if comets of QC 4 are discarded). The only exceptions for which $f > 1$ are: all the measurements of the water production rate of 21P/Giacobini–Zinner (comet of QC 3), one of the measurements of 24P/Schaumasse (comet of QC 4), and another one of 73P/Schwassmann–Wachmann 3 right after the comet split. As expected in the later case, the measured Q_{H_2O} was extremely high which led to an absurd $f \gg 1$. In physical terms it should be interpreted as the sublimation of water from a large number of ice-rich fragments released from the parent nucleus after the splitting. In the other cases we note that the uncertainties

in the computed area due to the bad quality classes of our derived magnitudes, are enough to bring the values of the fraction below 1. Unreported minor outburst and minor splitting events could also explain this large fraction values.

The largest comet in the sample, 28P/Neujmin 1 ($R_N = 9.58$ km), exhibits a very small fraction of active surface area (0.1%), but the sample is still too small to assess whether this is a general property of large comet nuclei. The few comets in our sample larger than $R_N \sim 3$ km have fractions $f \lesssim 0.01$. On theoretical grounds (e.g., Rickman et al., 1990), we should expect that large comet nuclei are more capable of building insulating dust mantles that choke off gas sublimation to very low levels. In any case, if very small f values characterize all comets with $R_N \gtrsim 3$ km, we may expect a change in the exponent of the size distribution at $R_N \sim 3$ km, because the capability of larger comet nuclei of building insulating dust mantles may prolong their physical survival.

A few cautionary comments are in order. As explained, the radii of the comet nuclei were derived by adopting a canonical geometric albedo, usually $p_V = 0.04$. But as discussed in Section 5, we know that there are variations in p_V among different comets. We also note that the nucleus radius $R_N \propto p_V^{-1/2}$, so a change in albedo will correspond to a change in $f \propto p_V$. However, a more substantial uncertainty of f may come from the uncertainty of the nuclear magnitude (and thus radius), especially for comets of QC 3 or 4.

There are also modeling uncertainties involved in the computation of $Z(r)$. Those do not concern the assumption of a
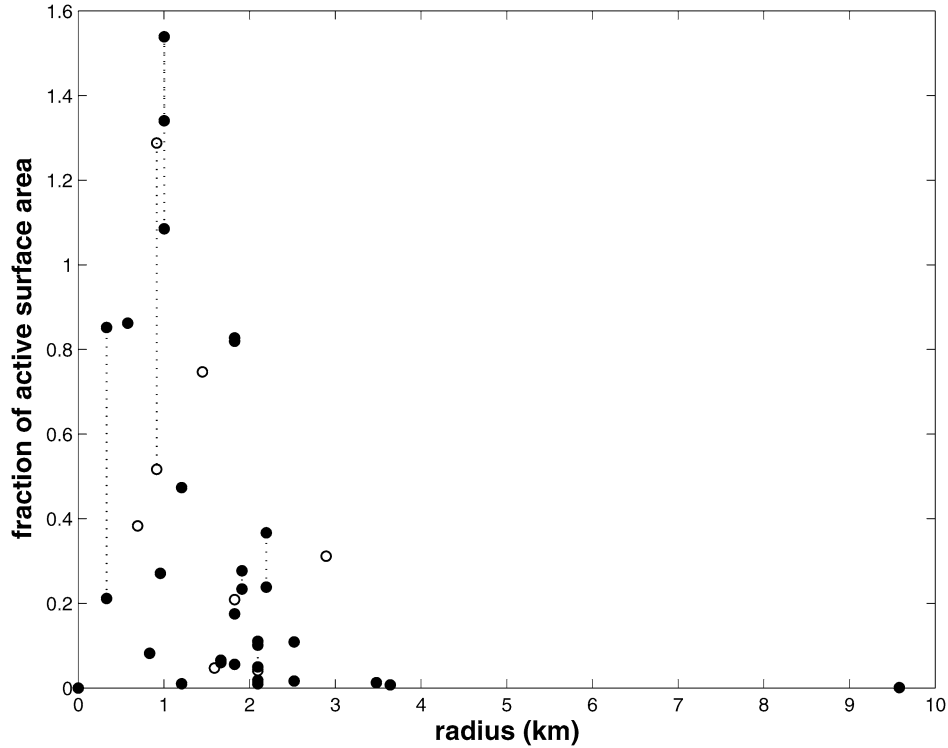
Fig. 16. Computed fraction of free-sublimating area versus the radius of the comet nucleus for an assumed geometric albedo $p_V = 0.04$ (as shown in Table 1). Filled circles are for comets of QC 3 or better, while open circles are for comets of QC 4.

very low visual Bond albedo, which is safe, because of the observational evidence for low geometric albedos, and inconsequential, since the outgassing flux is insensitive to the value assumed. However, the use of a classical surface energy balance is not self-evident and has been applied only because it allows simple estimates to be made independent of the detailed properties of the nucleus. If we would use the Layer Energy Absorption Model of Davidsson and Skorov (2002), the water fluxes would be lower and the f values would increase. An example of models for Comet 67P/Churyumov–Gerasimenko can be found in a recent paper by Davidsson and Gutiérrez (2005). Finally, concerning the occurrence of f values near the upper bound of unity, and the possibility that some of them might even be underestimates, let us note that the phenomenon invoked to explain the very large f of 73P after its splitting might also be present to a lower extent in other comets. For the case of 46P/Wirtanen, see Rickman and Jorda (1998).

8. Discussion

The sample of JF comets with reliable absolute nuclear magnitudes has grown substantially in the last few years, so we are now able to discuss on better grounds important properties, such as the size distribution and the fraction of active surface area. Though we have size estimates down to a few hundred meters, we observe an important depletion at sizes smaller than $R_N \sim 1.5$ km (absolute magnitude brighter than $H_N \sim 16.7$). If this depletion is just due to a selection effect or to some physical process that rapidly destroys small comets, is still an open question that we will not be able to answer until more size es-

timates of small comets can be obtained. The topic of the size distribution of comets has been very active in recent years, with at least five different groups that made compilations of size estimates. From the different studies it is clear that the cumulative size distribution of JF comets follows a power law, but the value of the index has been a matter of dispute. After a detailed analysis of the different compilations of size estimates including an update of our own values, we conclude that the size distribution down to a size limit of $R_N \sim 1.5$ km follows a power-law with an exponent $s = -2.7 \pm 0.3$. As discussed, our resulting index for the power law CSD (in modulus) is larger than those found by other groups. We are able to explain this discrepancy in terms of the different weights given to the largest members of the sample, the different criteria to define a JF comet, the inclusion of other categories of objects, the disagreement in some estimated comet magnitudes and/or the estimate of the turn-off point of the CSD. But, after applying a common definition to all the data sets, a common procedure to treat the data and to compute the slope index and allowing for the previous effects, we have been able to obtain similar results for the index s.

The value of $s = -2.7 \pm 0.3$ is in agreement with what may be expected from a collisional origin in the source region. It is also very close to the index for the size distribution found for trans-neptunian objects (TNOs). This might be just a simple coincidence, but it might be that JF comets come from the Edgeworth–Kuiper belt or the scattered disk and that the physical erosion suffered by comet nuclei as they reached the region interior to Jupiter's orbit had little effect in changing the original size distribution. Yet, caution should be

taken when comparing the size distribution of JF comets and TNOs since the size ranges covered by the derived size distribution are quite different (100-km size for TNOs, and km-size for JFCs).

By combining the nucleus size with the gas production rate we are able to obtain the fraction of free sublimation surface area. We find that about 60% of the JF comets of our sample have fractions <0.2, in agreement with the small fractions of active area found in 1P/Halley, 19P/Borrelly, 81P/Wild 2, and 9P/Tempel 1 during flybys (judging from the measured nuclear sizes and gas production rates). There is a hint of a possible correlation of the fraction of active surface area with the nucleus size, but we still have too few large comets to draw a firm conclusion in this regard.

References

A'Hearn, M.F., Millis, R.L., Schleicher, D.G., Osip, D.J., Birch, P.V., 1995. The ensemble properties of comets: Results from narrowband photometry of 85 comets, 1976–1992. Icarus 118, 223–270.

A'Hearn, M.F., Belton, M.J.S., Delamere, W.A., Kissel, J., Klaasen, K.P., Mc-Fadden, L.A., Meech, K.J., Melosh, H.J., Schultz, P.H., Sunshine, J.M., Thomas, P.C., Veverka, J., Yeomans, D.K., Baca, M.W., Busko, I., Crockett, C.J., Collins, S.M., Desnoyer, M., Eberhardy, C.A., Ernst, C.M., Farnham, T.L., Feaga, L., Groussin, O., Hampton, D., Ipatov, S.I., Li, J.-Y., Lindler, D., Lisse, C.M., Mastrodemos, N., Owen Jr., W.M., Richardson, J.E., Wellnitz, D.D., White, R.L., 2005. Deep Impact: Excavating Comet Tempel 1. Science 310, 258–264.

Bernstein, G.M., Trilling, D.E., Allen, R.L., Brown, M.E., Holman, M., 2004. The size distribution of trans-neptunian bodies. Astron. J. 128, 1364–1390.

Binzel, R., Rivkin, A., Stuart, J., Harris, A., Bus, S., Burbine, T., 2004. Observed spectral properties of near-Earth objects: Results for population distribution, source regions, and space weathering processes. Icarus 170, 259–294.

Brownlee, D.E., and 11 colleagues, 2004. Surface of young Jupiter family Comet 81 P/Wild 2: View from the Stardust spacecraft. Science 304, 1764–1769.

Buratti, B.J., Hicks, M.D., Soderblom, L.A., Britt, D., Oberst, J., Hillier, J.K., 2004. Deep Space 1 photometry of the nucleus of Comet 19P/Borrelly. Icarus 167, 16–29.

Campins, H., Fernández, Y., 2002. Observational constraints on surface characteristics of comet nuclei. Earth Moon Planets 89, 117–134.

Campins, H., A'Hearn, M.F., McFadden, L.-A., 1987. The bare nucleus of Comet Neujmin 1. Astrophys. J. 316, 847–857.

Campins, H., Osip, D.J., Rieke, G.H., Rieke, M.J., 1995. Estimates of the radius and albedo of comet–asteroid transition object 4015 Wilson–Harrington based on infrared observations. Planet. Space Sci. 43, 733–736.

Carusi, A., Kresák, L., Perozzi, E., Valsecchi, G.B., 1987. High-order librations of Halley-type comets. Astron. Astrophys. 187, 899–905.

Crovisier, J., Colom, P., Gérard, E., Bockelée-Morvan, D., Bourgois, G., 2002. Observations at Nançay of the OH 18-cm lines in comets. The data base. Observations made from 1982 to 1999. Astron. Astrophys. 393, 1053–1064.

Davidsson, B.J.R., Gutiérrez, P.J., 2005. Nucleus properties of Comet 67P/Churyumov–Gerasimenko estimated from non-gravitational force modeling. Icarus 176, 453–477.

Davidsson, B.J.R., Skorov, Yu.V., 2002. On the light-absorbing surface layer of cometary nuclei. II. Thermal modeling. Icarus 159, 239–258.

Delahodde, C.E., Meech, K.J., Hainaut, O.R., Dotto, E., 2001. Detailed phase function of Comet 28P/Neujmin 1. Astron. Astrophys. 376, 672–685.

Duncan, M., Quinn, T., Tremaine, S., 1988. The origin of short-period comets. Astrophys. J. 328, L69–L73.

Fernández, J.A., 1980. On the existence of a comet belt beyond Neptune. Mon. Not. R. Astron. Soc. 192, 481–491.

Fernández, J.A., Tancredi, G., Rickman, H., Licandro, J., 1999. The population, magnitudes, and sizes of Jupiter family comets. Astron. Astrophys. 352, 327–340.

Fernández, Y.R., Lisse, C.M., Käufl, U.H., Peschke, S.B., Weaver, H.A., A'Hearn, M.F., Lamy, P.P., Livengood, T.A., Kostiuk, T., 2000. Physical properties of the nucleus of Comet 2P/Encke. Icarus 147, 145–160.

Fernández, J.A., Gallardo, T., Brunini, A., 2002. Are there many inactive Jupiter-family comets among the near-Earth asteroid population? Icarus 159, 358–368.

Fernández, Y.R., Meech, K.J., Lisse, C.M., A'Hearn, M.F., Pittichová, J., Belton, M.J.S., 2003. The nucleus of Deep Impact target Comet 9P/Tempel 1. Icarus 164, 481–491.

Fink, U., Hicks, M.D., 1996. A survey of 39 comets using CCD spectroscopy. Astrophys. J. 459, 729–743.

Gladman, B., Kavelaars, J.J., Petit, J.-M., Morbidelli, A., Holman, M.J., Loredo, T., 2001. The structure of the Kuiper belt: Size distribution and radial extent. Astron. J. 122, 1051–1066.

Gutiérrez, P.J., Rodrigo, R., Ortiz, J.L., Davidsson, B.J.R., 2003. An investigation of errors in estimates of the cometary nuclei active area fractions. Astron. Astrophys. 401, 755–761.

Hartmann, W.K., Tholen, D.J., Cruikshank, D.P., 1987. The relationship of active comets, "extinct" comets, and dark asteroids. Icarus 69, 33–50.

Jedicke, R., Metcalfe, T.S., 1998. The orbital and absolute magnitude distributions of main belt asteroids. Icarus 131, 245–260.

Jewitt, D., Luu, J., 1989. A CCD portrait of Comet P/Tempel 2. Astron. J. 97, 1766–1790.

Jewitt, D., Meech, K.J., 1985. Rotation of the nucleus of Comet P/Arend–Rigaux. Icarus 64, 329–335.

Jewitt, D., Meech, K.J., 1988. Optical properties of cometary nuclei and a preliminary comparison with asteroids. Astrophys. J. 328, 974–986.

Jewitt, D., Sheppard, S., 2004. The nucleus of Comet 48P/Johnson. Astron. J. 127, 1784–1790.

Jewitt, D., Trujillo, C., Luu, J., 2000. Population and size distribution of small jovian trojan asteroids. Astron. J. 120, 1140–1147.

Jewitt, D., Sheppard, S., Fernández, Y., 2003. 143P/Kowal–Mrkos and the shapes of cometary nuclei. Astron. J. 125, 3366–3377.

Kamél, L., 1991. The comet light curve catalogue/atlas. I. The compiled observations. Ph.D. thesis, Uppsala Universitet Reprocentralen HSC, Uppsala, Sweden.

Kenyon, S.J., Bromley, B.C., 2004. The size distribution of Kuiper belt objects. Astron. J. 128, 1916–1926.

Kührt, E., Keller, H.U., 1994. The formation of cometary surface crusts. Icarus 109, 121–132.

Lamy, P.L., Toth, I., Jorda, L., Groussin, O., A'Hearn, M.F., Weaver, H.A., 2002. The nucleus of Comet 22P/Kopff and its inner coma. Icarus 156, 442–455.

Lamy, P.L., Toth, I., Fernández, Y.R., Weaver, H.A., 2005. The sizes, shapes, albedos, and colors of cometary nuclei. In: Festou, M.C., Keller, H.U., Weaver, H.A. (Eds.), Comets II. Univ. of Arizona Press, Tucson, pp. 223–264.

Levison, H.F., 1996. Comet taxonomy. In: Rettig, T.W., Hahn, J.M. (Eds.), Completing the Inventory of the Solar System. In: ASP Conf. Ser., vol. 107. Astron. Soc. Pacific, pp. 173–191.

Levison, H.F., Duncan, M.J., 1997. From the Kuiper belt to Jupiter-family comets: The spatial distribution of ecliptic comets. Icarus 127, 13–32.

Licandro, J., de León, J., Pinilla-Alonso, N., Serra-Ricart, M., 2005. Physical nature of asteroids in cometary orbits (ACOs). Adv. Space Res. In press.

Lowry, S.C., Fitzsimmons, A., Collander-Brown, S., 2003. CCD photometry of distant comets. III. Ensemble properties of Jupiter-family comets. Astron. Astrophys. 397, 329–343.

Luu, J., Jewitt, D., 1990. The nucleus of Comet P/Encke. Icarus 86, 69–81.

Luu, J.X., Jewitt, D.C., 1992. Near-aphelion CCD photometry of Comet P/S Schwassmann–Wachmann 2. Astron. J. 104, 2243–2249.

Mäkinen, J.T.T., Silén, J., Schmidt, W., Kyrölä, E., Summanen, T., Bertaux, J.-L., Quémerais, E., Lallement, R., 2001. Water production of Comets 2P/Encke and 81P/Wild 2 derived from SWAN observations during the 1997 apparition. Icarus 152, 268–274.

Meech, K.J., Hainaut, O.R., Marsden, B.G., 2004. Comet nucleus size distributions from HST and Keck telescopes. Icarus 170, 463–491.

Millis, R.L., A'Hearn, M.F., Campins, H., 1988. An investigation of the nucleus and coma of Comet P/Arend–Rigaux. Astrophys. J. 324, 1194–1209.

Neslušan, L., 2003. Observed sizes of cometary nuclei. A summary. Contrib. Astron. Obs. Skalnaté Pleso 33, 5–20.

Newburn Jr., R.L., Spinrad, H., 1989. Spectrophotometry of 25 comets—Post-Halley updates for 17 comets plus new observations for eight additional comets. Astron. J. 97, 552–569.

Rabinowitz, D.L., 1993. The size distribution of the Earth-approaching aster-oids. Astrophys. J. 407, 412–427.

Rickman, H., Jorda, L., 1998. Comet 46P/Wirtanen, the target of the Rosetta mission. Adv. Space Res. 21 (11), 1491–1504.

Rickman, H., Fernández, J.A., Gustafson, B.Å.S., 1990. Formation of stable dust mantles on short-period comet nuclei. Astron. Astrophys. 237, 524–535.

Soderblom, L.A., and 21 colleagues, 2002. Observations of Comet 19P/Borrelly by the Miniature Integrated Camera and Spectrometer aboard Deep Space 1. Science 296, 1087–1091.

Svoreň, J., 1987. Consequences of the size determination of P/Halley by space probes on the scale of sizes of cometary nuclei. In: Proceedings of the International Symposium on the Diversity and Similarity of Comets, ESA SP-278, pp. 707–712.

Tancredi, G., Fernández, J.A., Rickman, H., Licandro, J., 2000. A catalog of observed nuclear magnitudes of Jupiter family comets. Astron. Astrophys. Suppl. Ser. 146, 73–90.

Valsecchi, G.B., 1992. First round table: Dynamics of periodic comets. In: Fernández, J.A., Rickman, H. (Eds.), Periodic Comets. Univ. República, Montevideo, Uruguay, p. 98.

Weissman, P.R., Lowry, S.C., 2003. The size distribution of Jupiter-family cometary nuclei. Lunar Planet. Sci. 34. Abstract 2003.